BD

STRUCTURAL AND STRAIN ANALYSIS OF THE NOSE OF THE MYPONGA-LITTLE GORGE INLIER, FLEURIEU PENINSULA, SOUTH AUSTRALIA

by

J. A. Anderson, B.Sc.

Submitted as part of the requirements for the
Honours Degree of Bachelor of Science.
Department of Geology and Mineralogy
University of Adelaide.

November, 1975.

TABLE OF CONTENTS

		Page
	ABSTRACT	
1.	INTRODUCTION	1
	1.1 General Geology	1
	1.2 Methods of Investigation	2
	1.3 Physiography	2
2.	NATURE OF THE REGIONAL RECLINED FOLD	4
	2.1 Cover Stratigraphy	4
	2.2 Closure of the Regional Overturned Fold	5
	2.3 Position of the Axial Trace	7
	2.4 Orientation of the Regional Fold Axis	7
3.	MICROSTRUCTURE OF THE COVER AND BASEMENT LITHOLOGIES	9
	3.1 Regional Metamorphism	9
	3.2 F_1 Tectonothermal Microstructure	10
	3.3 Nature of the Deformation associated with the Fabric Formation	11
4.	RELATIONSHIP OF FABRICS TO DEFORMATION	13
	4.1 Foliation	13
	4.2 Lineation	13
	4.3 Macroscopic Variation in Fabric Orientation	13
	4.4 Nature and Orientation of the Simple Shear Model	14
5.	STRAIN ANALYSIS OF PEBBLES AND QUARTZ GRAINS	16
	5.1 Nature of the Basal Conglomeratic Arkosic Sandstone	16
	5.2 Methods of Measurement	18
	5.3 Rf/Ø Diagram Analysis	19
	5.4 Suitability of Rf/Ø Diagram Analysis	20
	5.5 Results of Rf/Ø Diagram Strain Analysis	21
	5.6 Es and V Estimates	23
	5.7 Variation in the Finite Strains	24
	5.8 Regional Distribution of Strains	25
	5.9 Discussion of Strain Results	26
6.	LATER DEFORMATIONS	30
	6.1 Crenulation Cleavage and Lineation	30
	6.2 Conjugate Faulting and Associated Fold Development	30
7.	CONCLUSIONS	32
	7.1 General	32
	7.2 Nature of Deformation	32

TABLE OF CONTENTS (cont'd)

	Page
7.3 Relationship of Fold Formation to Elongation Lineation Development	33
7.4 Recommendations	34
ACKNOWLEDGEMENTS	35
BIBLIOGRAPHY	36
APPENDIX 1 - THIN SECTION DESCRIPTIONS	40
APPENDIX 2 - TABULATED DESCRIPTION OF SAMPLES USED FOR QUARTZ GRAIN STRAIN ANALYSIS.	45

NOMENCLATURE

X,Y,Z - Principal axes of the triaxial strain ellipsoid. $X \geqslant Y \geqslant Z$

Rf - Final deformed ellipse axial ratio in a principal plane.

Rs - Finite strain axial ratio.

Ri - Initial undeformed particle axial ratio.

ϕ - Angle between the Rf long axis and the maximum principal strain direction in the principal plane considered.

θ - Angle between the Ri long axis and the maximum principal strain direction.

$\bar{E}s$ - An absolute measure of the magnitude of the distortional component of strain. $\bar{E}s$ is directly proportional to the natural octahedral shear ($\bar{\gamma}_o$).

V - Lodes unit. A measure of deformation symmetry.

k - Flinns k. An alternative measure of deformation symmetry.

γ - Magnitude of shear strain.

θ' - Angle of planar fabric dip in the right section to strike.

ABSTRACT

The Myponga-Little Gorge Inlier is the core of a regional reclined fold, which is delineated by the stratigraphy of the Adelaidean cover and by detailed structural analysis. The regional fold formation occurred during the F_1 phase of the Palaeozoic Delamerian Orogeny. The regional fold axis is orientated with a shallow southeast plunge which is perpendicular to the regional trend. Although the fold closure is to the southwest, brittle thrusting disrupts the nose of the inlier.

Planar zones of extensive phyllonitization and foliation development in basement lithologies adjacent to the overturned basement-cover contact, are interpreted as zones of simple shear. Formation of these zones is considered contemporaneous with the development of an elongation lineation, which is reflected by deformed pebbles and clastic grains in the basal conglomeratic sandstone.

A quantitative strain analysis of the conglomerate is discussed. Deformation paths interpreted from the variation of finite strains suggest prolate strains have developed from less significant oblate strains. This is inconsistent with the plane strains inferred by the proposed simple shear model. Two possible explanations are considered likely:
(a) As Rf/Ø diagram analysis suggests that only one deformation has been imposed on an initial sedimentary fabric, the finite strain variation may not represent a true deformation path, which is a result of two deformations. Therefore plane strain and the simple shear model may be valid.
(b) The estimates of prolate strains may be realistic, in which case, the simple shear model is invalid.

The F_2 phase of the Delamerian Orogeny is represented by a small-scale crenulation cleavage and lineation. Widespread but insignificant conjugate faulting also post-dates the regional fold formation.

1. INTRODUCTION

1.1 General Geology

Within the Mount Lofty Ranges, several inliers of the Barossa Complex (Thomson, 1966) form the cores of overturned regional anticlinal structures, which are dislocated by shearing on the western limbs. The inliers act as basement to the unconformably overlying Adelaide Supergroup (Daily, 1963). This Adelaidean sequence is thought to be Upper Proterozoic in age as it is unconformably overlain by Lower Cambrian fossiliferous sediments (Abele and McGowran, 1959). Upper to Middle Proterozoic radiometric ages have been obtained for the basement lithologies within the inliers and also for their equivalents on Yorke Peninsula (Compston et al., 1966; Cooper and Compston, 1971).

Radiometric dating indicates an age of 465 million years for the major orogenesis in the Adelaide Geosyncline (Compston et al. (op. cit.)). Offler and Fleming (1968) attribute three phases of folding to the orogeny, of which the first phase (F_1) resulted in the major overturned anticlinal and reclined folds with the basement as core inliers. The inliers are exposed in the lower greenschist facies zones defined by Offler and Fleming for the post-basement lithologies. Convergent retrogression of initially high grade amphibolite facies basement to equivalent low metamorphic grades, has resulted in obliteration of the early basement structures by phyllonitization (Talbot, 1964).

Daily and Milnes (1971b, 1972a) and Stuart and von Sanden (1972) have described and recognized the significance of the thrusts and reverse faults associated with overturned regional anticlines.

The subject of this thesis is a study of the southwest continuation of the Myponga-Little Gorge Inlier on the northwest coast of the Fleurieu Peninsula, forty miles south of Adelaide, South Australia (Figure 1). The nature of the brittle thrusting and proposed ductile

FIGURE 1. LOCATION MAP

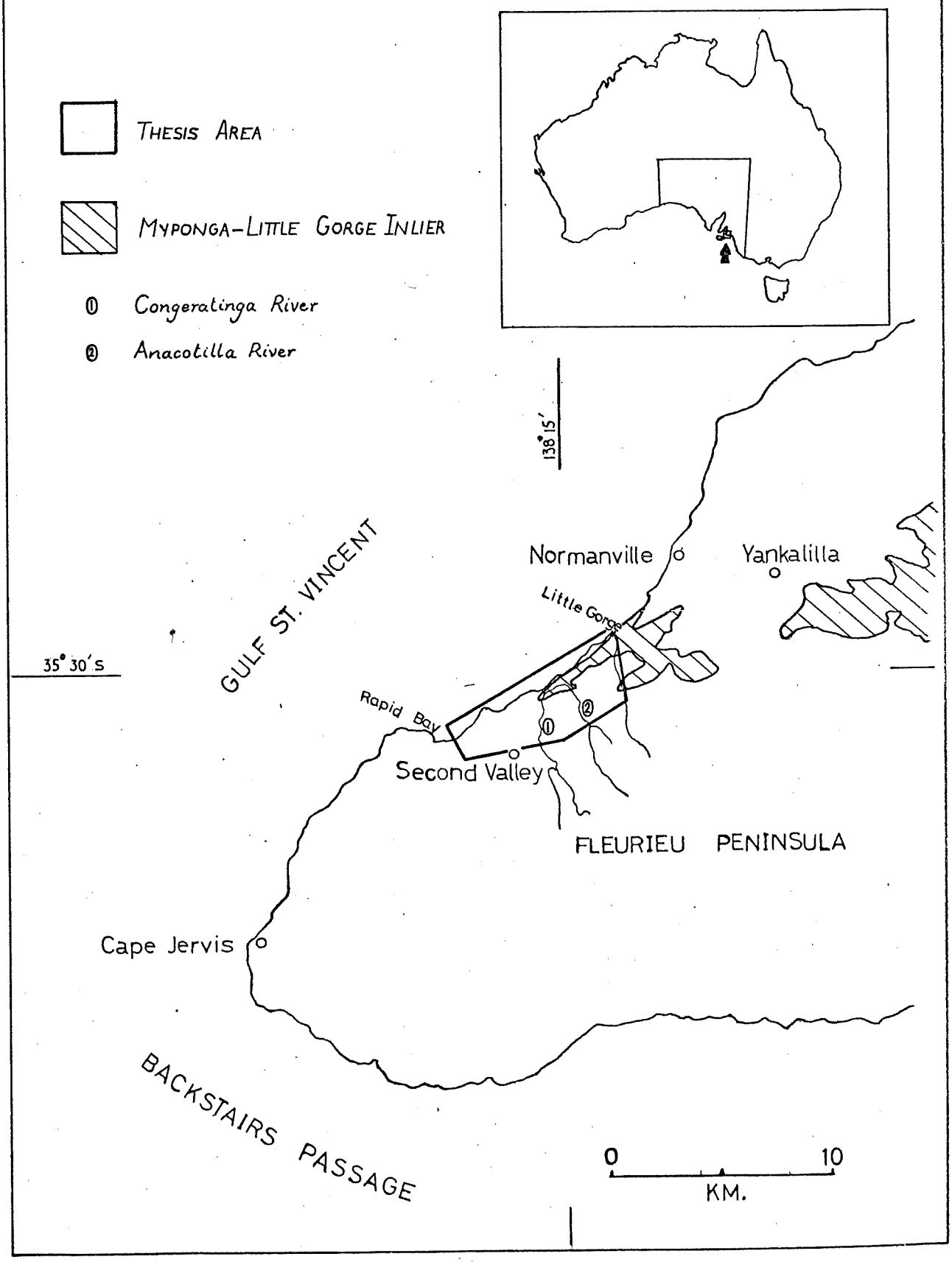

shearing is examined with respect to the orientation and nature of the regional fold structure which has the basement inlier as a core.

Campana et al. (1953) associated thrusting with the overturned basement-cover contact. They considered the regional fold to be an overturned anticline which plunges to the southwest. However Robinson (1962) and Offler and Fleming (op.cit.) accept that the fold is reclined and plunges to the southeast, parallel to the mesoscopic fold axes.

Abele and McGowran (1959) describe pre-Permian thrusting along the northeast-southwest trending Black Hill Fault in Cambrian sediments near Carrackalinga Head, which is immediately northeast of the area studied. Drayton (1962) also delineates a fault of similar trend in the Rapid Bay region to the south. A number of post-folding and post-metamorphic thrust wrench faults have been defined by Mills in the Kanmantoo Group on the east side of the Mount Lofty Fold Belt (Forbes, 1966).

Shearing adjacent to the basement-cover contact on the overturned limbs has been proposed by Davies (1972) and McEwin (1972) for the Myponga-Little Gorge Inlier and by Talbot (1963) in the Houghton Inlier. The shearing is associated with phyllonitization of both the basement and cover lithologies.

1.2 Methods of Investigation

Interpretive and qualitative analysis of the Delamerian fold, shear and thrust deformations were initially conducted by lithological and structural mapping of the area bounded by the coastline and the Normanville-Cape Jervis road between Second Valley and Little Gorge (Figure 1). Petrological examination and quantitative studies of natural finite strains estimated from pebble and grain clast shapes; mesoscopic fold orientations and macroscopic fabric variations are also described.

1.3 Physiography

Wave-cut beach platforms and continuous coastal cliffs over

200 metres high, expose good outcrop as do the steeply graded streams which have produced a moderate inland relief by dissecting the uplifted pre-Tertiary peneplane surface. The Anacotilla and Congeratinga Rivers expose the basement inlier and cover in the vicinity of the nose of the Myponga-Little Gorge Inlier. Elsewhere the outcrop is extremely poor and disconnected as a result of cappings of leached residual soils and Permian morainic material, in addition to the scree, alluvium and soil which cover the lower slopes and flats.

Pastoral farming activities have removed most of the natural scrub vegetation, leaving only large eucalyptus gums in the watercourses.

2. NATURE OF THE REGIONAL RECLINED FOLD

2.1 Cover Stratigraphy

The predominant bedding orientation of the Adelaidean cover units parallels the regional foliation, which strikes southwest with moderate to shallow southeasterly dips (Plate 2; A,B,C,D). This is consistent with the major trend of the Adelaide Fold Belt. The regional fold has been recognized by the repetition of the cover stratigraphy on each side of the basement inlier (Sprigg and Campana, 1953). Therefore the foliation development is axial plane to the fold.

Consistent sedimentary facings in the basal cover units indicate that the stratigraphy is west facing and overturned on the western side of the inlier and upward facing on the eastern flank. As graded bedding is often reversed, abundant truncated cross bedding is the most reliable indicator.

Robinson (1962) describes the stratigraphy in detail and a reinterpreted stratigraphic column is shown in figure 2.

A basal conglomeratic and heavy mineral banded, gritty, arkosic sandstone is correlated with the Aldgate Sandstone of the Burra Group. This unit is overlain by a sequence of medium grained, buff, dolomitic sandstones and dark phyllitic siltstones grading into green-brown, indurated, layered slates with thick, blue-grey, bedded or light grey, massive quartzite interbeds. The boundaries between the three units are transitional and the sequence is correlated with the Burra Group of Torrensian age.

Conformably overlying the Burra Group, the Sturt Tillite is represented by a prominent glacifluvial conglomerate with granules and pebbles of banded gneiss and quartzite over 50 centimetres in diameter. There lie supported by a matrix of grey to brown, non-stratified, argillaceous and calcareous siltstone. Thin, indurated, fine quartzite and dolomite interbeds occur within the unit.

FIGURE 2 STRATIGRAPHY OF THE ADELAIDEAN COVER

(Adapted from Robinson, 1962)

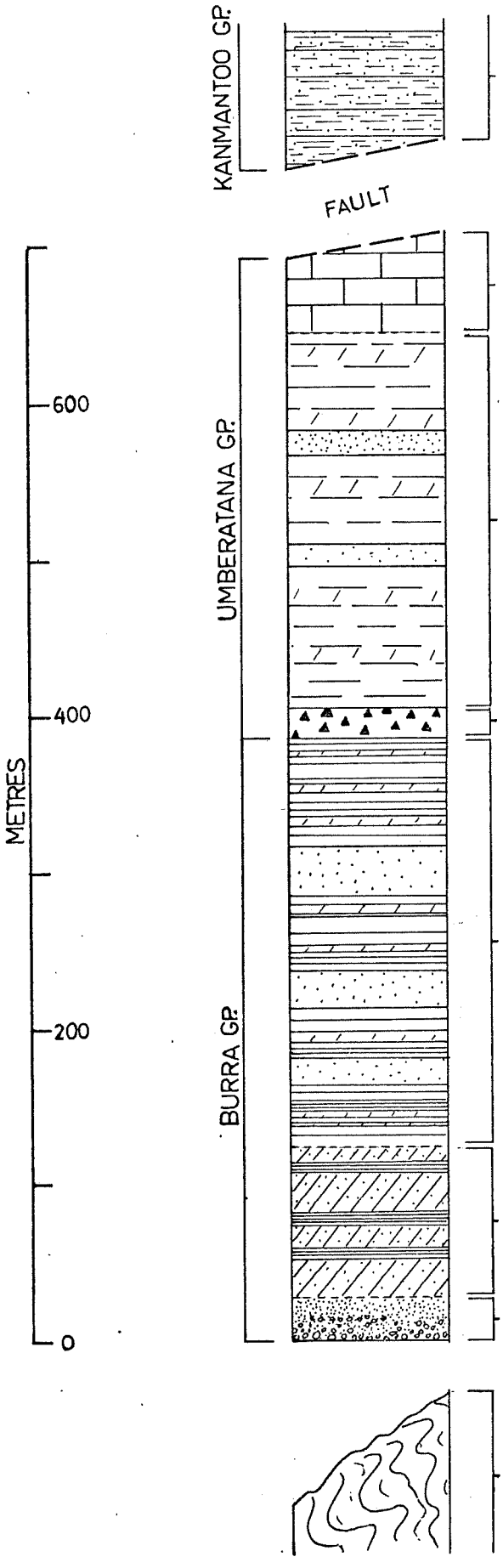

Thinly bedded, fine, pyritic and micaceous sandstones.

Lensoidal, banded blue grey and grey brown limestone. BRIGHTON LIMESTONE

Black to dark grey, calcareous, phyllitic coarse siltstone with interbeds of coarse feldspathic sandstone and massive quartzite. TAPLEY HILL FORM.

Grey to brown, non-stratified, argillaceous, calcareous siltstone. Pebbles and granules of gneiss and quartzite. STURT TILLITE

Brown to green, indurated, layered siltstones and fine sandstones. Interbeds of blue-grey, bedded or white massive quartzite.

Cream to buff dolomitic sandstone with dark grey phyllitic siltstone interbeds.

Coarse arkosic sandstone with prominent heavy mineral banding. Conglomeratic at base. ALDGATE SANDSTONE

BAROSSA COMPLEX - Chlorite, sericite, biotite augen schists; quartz, feldspar biotite epidote gneissic schists; pegmatites.

A thick sequence of the Tapley Hill Formation overlies the Sturt Tillite with a marked change in lithology. Dark grey to black, variably calcareous, coarse, phyllitic metasilts contain rare thick interbeds of coarse, feldspathic sandstones and massive quartzite. The contact of the phyllites with the Sturt Tillite may be a slight disconformity as interbeds in the latter are cut off at an acute angle by the contact, immediately south of the Congeratinga River outlet. With increasing carbonate content, the phyllite grades upwards into lensoidal, thinly interbanded, coarse blue-grey and fine brown grey limestones, which are correlated with the Brighton Limestone. The Sturt Tillite, Tapley Hill Formation and the Brighton Limestone comprise the Umberatana Group.

The lithologies outcropping above the Umberatana Group lithologies in the Congeratinga and Anacotilla Rivers are correlated with the Kanmantoo Group. They are thinly bedded, fine pyritic and micaceous sandstones. A fault contact between the two lithologies is suggested. This contact aligns with the continuation of the Nairne Fault (Kleeman and White, 1959) proposed by Daily to explain the contact between the Kanmantoo Group lithologies and the basement in the creek which flows through Little Gorge in the northern part of the area.

2.2 Closure of the Regional Overturned Fold

Sprigg and Campana (1953), Campana et al. (1953) and Robinson (1962) describe the closure of the Adelaidean cover units around the nose of the basement inlier in the vicinity of the Congeratinga River outlet. Evidence of the closure was based largely on the apparent closure of the prominent Sturt Tillite and Aldgate Sandstone (Plate 1).

Although Robinson inferred the existence of brittle faults in the area, both he and Campana et al. (op.cit.) did not recognize the extent of the discontinuities in the cover units due to brittle

faulting. Two continuous wrench thrust faults which were observed by Daily (1963, footnote), translate the basement-cover contact over a maximum lateral distance of 2½ kilometres, subparallel to the axial plane of the fold (Plate 1). The fault planes are orientated with a strike of approximately 210 degrees and a dip of 45 degrees to the southwest. Numerous microfaults, which subparallel the two major fault planes, contain quartz veins which consist of preferred, quartz fibre growth with a significant downdip component. In many cases, the microfaults are small scale thrust wrench faults.

Consequently, the closure of the basal conglomeratic and arkosic sandstone mapped previously, is only an apparent one, as the "nose" consists of two thrust slices of east limb which converge on either side of the upper fault plane (Plate 1). This situation led Daily (1963) to suggest a possible regional fold closure to the north-east by stratigraphic studies in the Rapid Bay-Delamere region.

Immediately north of Second Valley, the closure of the Sturt Tillite mapped by Sprigg and Campana (op.cit.) is not observed although the two limbs of the unit do progressively approach each other to the south until obscured by alluvium. The closures of calcareous and quartzite units mapped southwest of Second Valley are considered to be unrealistic.

Additional evidence of a south western closure for the regional fold is obtained from cleavage-bedding relationships and the vergence of the parasitic small-scale macroscopic and mesoscopic folds (Plate 2). The orientation of the bedding relative to the cleavage is consistent with a southwest closure, particularly in the conglomerate in which the short limbs of mesoscopic folds are uncommon. Accordingly, the parasitic folds are predominantly sinistral in the west limb and dextral in the upward facing limb. The sense of small mesoscopic folds may oppose the predominant fold sense on the regional limbs, if located

on the short axes of larger asymmetrical mesoscopic folds.

An approximate reconstruction of the regional fold is made by translating the lithologies along the thrust planes to a position of coincidence of cleavage-bedding relationships and mesoscopic fold sense (Figure 3). High cleavage-bedding angles occur in the regional fold nose, but they generally approach zero in the limbs. Therefore the equal area stereoplot of the bedding poles is a point concentration (Plate 2).

2.3 Position of the Axial Trace

The position of the axial trace is determined by the broad change of the mesoscopic fold sense between the two limbs. The trace parallels the coastline with a slightly greater westerly trend than that of the major faulting (Plate 1). In the vicinity of Second Valley harbour, the axial trace position is difficult to determine due to a number of small scale faults and variable vergences resulting from the superposition of different scales of folds. However the projection of the axial trace to the south, passes through the Rapid Bay Area, where Drayton (1962) observed M and Z mesoscopic folds. The thickened sequence of Brighton Limestone in the proximity of the fold nose southwest of Second Valley, may continue as far as Rapid Bay. This would support the view (Daily, personal communication) that the Rapid Bay Limestone is equivalent to the Brighton Limestone.

2.4 Orientation of the Regional Fold Axis

Campana et al. (1953) initially described the regional fold as anticlinal, inferring a fold axis plunge to the southwest within the axial plane foliation. However the bedding and fold envelopes in the regional fold nose indicate a fold axis orientation which parallels the mesoscopic fold axes and elongation lineation orientations.

The fold structure is, therefore, now recognized as a southeast plunging reclined fold (Robinson, 1962; Offler and Fleming, 1968).

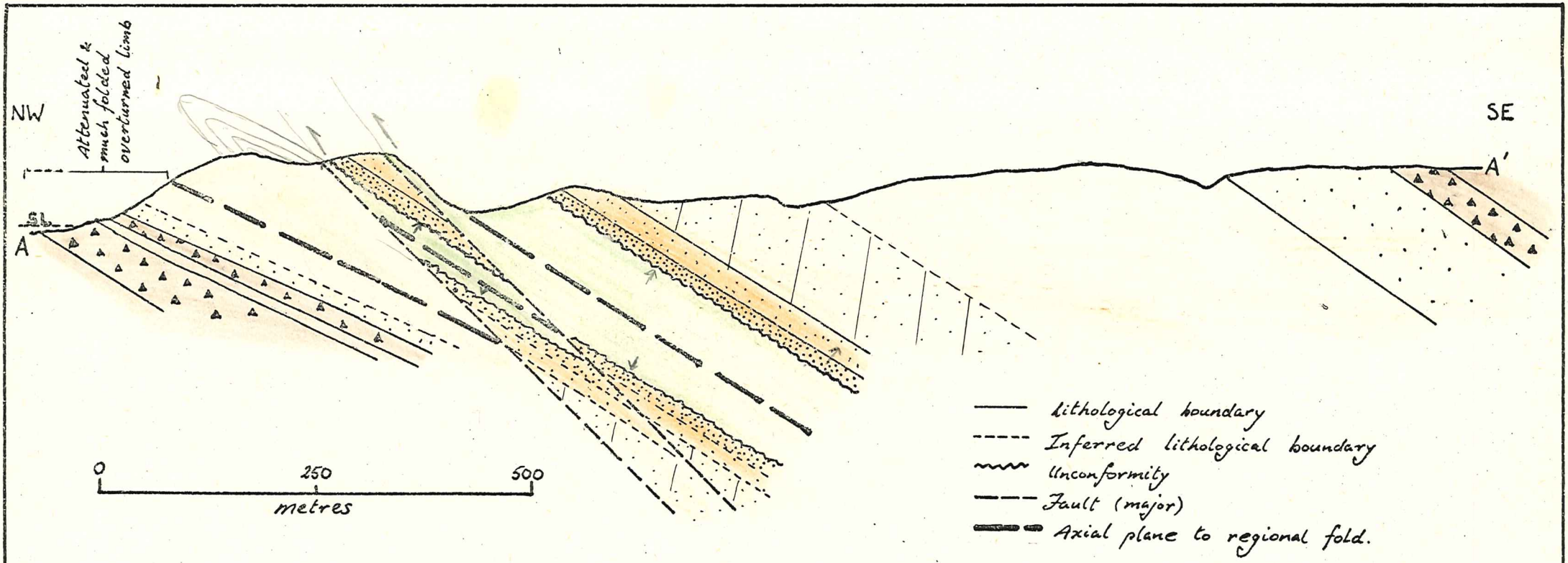

SECTION – *Vertical section along SW cliffs of Congeratinga River.*

A-A' on Plate 1. Topography and bedding dips approximate only. Vertical scale not exaggerated. Facing Northeast.

FIGURE 3 INTERPRETATION OF THE NATURE OF THE REGIONAL FOLD PRIOR TO THE BRITTLE THRUSTING

TRACE OF THRUSTS PRIOR TO MOVENT

ALDGATE SANDSTONE

STURT TILLITE

ZONES OF STEEP FABRIC DIP (greater than 50°)

ZONES OF SHALLOW FABRIC DIP (less than 20°)

VERTICAL CROSS-SECTION (Refer to figure 4)

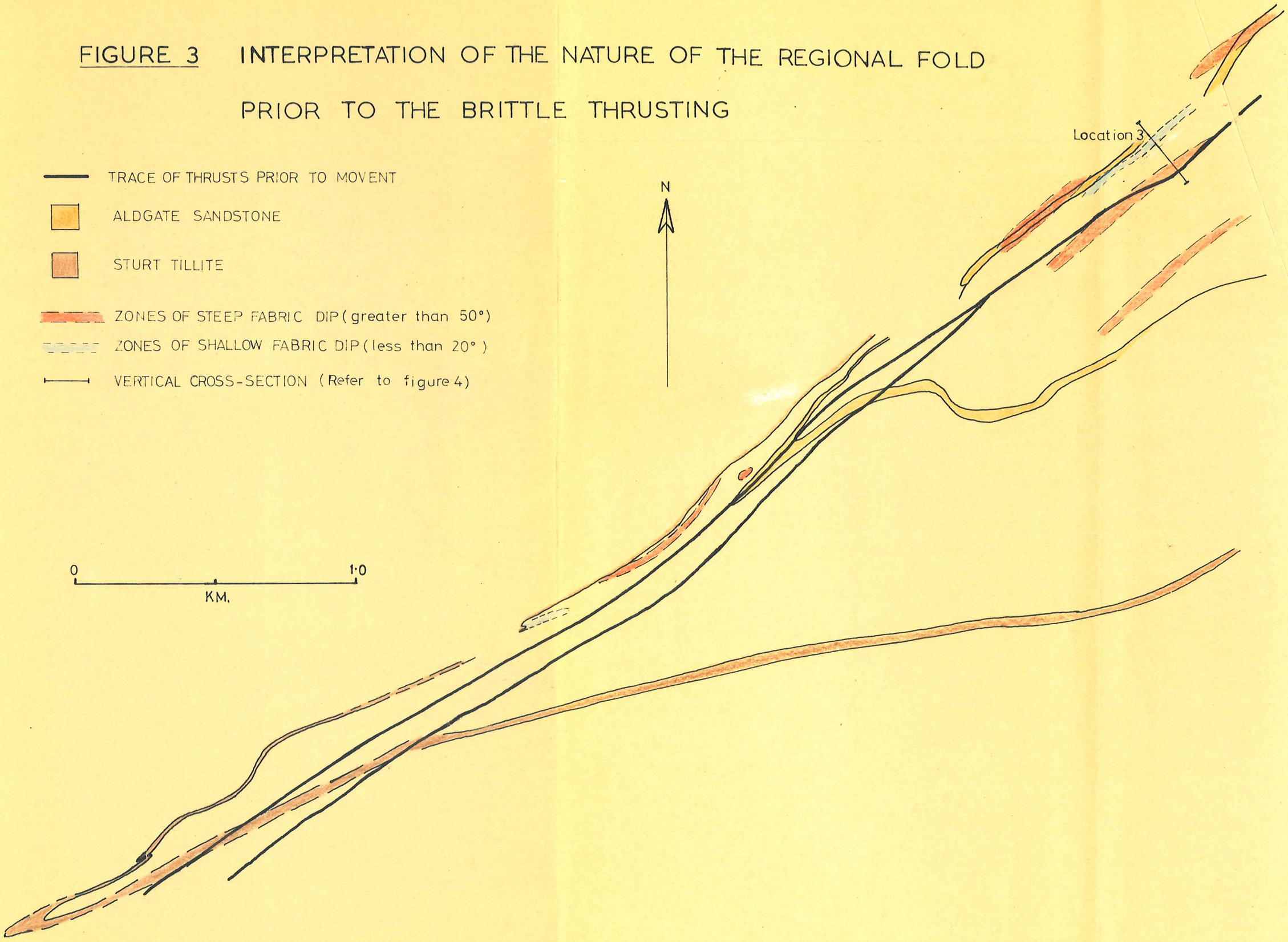

The macroscopic and mesoscopic fold axes and the bedding-cleavage intersections are sub-parallel to the elongation lineation, which is defined by stretched pebbles and clastic grains, as well as the streaking of micas (Plate 2). The orientation of the elongation lineation is relatively constant across the Adelaide Fold Belt, in contrast to the variable pitch of the F_1 fold axes within the axial plane schistosity. A current study of this variation in fold axes' orientation is being conducted by N. Mancktelow of the University of Adelaide. He suggests (personal communication) that the rotation of the fold axes within the axial planes may be progressive across the Fold Belt. Hence the relationship between the fold development and the elongation lineation may not be genetic.

A small number of mesoscopic folds are located in basement lithologies on the beach immediately south of Little Gorge. These folds, for which the foliation is axial plane, have variable steep to shallow plunges to the northeast. Their relationship with the folds which are sub-parallel to the elongation lineation, is difficult to determine. In view of the common axial plane for the two fold axes' orientations, they are considered to be genetically related. Two other folds observed in the basement, have fold axes which are sub-parallel to the elongation lineation.

3. MICROSTRUCTURE OF THE COVER AND BASEMENT LITHOLOGIES

3.1 Regional Metamorphism

The area studied lies within the biotite zone of the progressive metamorphic zoning of the metasilts and calcareous sediments defined by Offler and Fleming (1968). They associate the progressive cover metamorphism to the F_1 deformation which produced the regional folds. The presence of biotite, sericite and occasional chlorite in the cover units (Appendix 1, thin sections 1-4) verifies the zoning.

A high, pre-F_1 metamorphic grade of upper amphibolite facies has been proposed for the basement lithologies from the presence of relict sillimanite, garnet, diopside, scapolite and andalusite (Talbot, 1964; Davies, 1972; McEwin, 1972). A convergent retrogression of the basement lithologies to a lower greenschist facies during F_1 is indicated by the alteration of plagioclase, hornblende and garnet to sericite and epidote, epidote and chlorite respectively. No minerals of high metamorphic grade were positively identified by microscopic study of the basement lithologies within the nose of the inlier. Epidote, biotite and muscovite are the commonly observed minerals of the retrogressed assemblage (Appendix 1, thin sections 6-7).

Talbot (op.cit.) proposes two periods of greenschist metamorphism in the Houghton Complex, the first being pre-F_1 as the basement pebbles in the basal Torrensian conglomerate show a pre-depositional retrogression. Microscopic examination of the feldspathic quartzite pebbles in basal cover units adjacent to the Myponga-Little Gorge Inlier do not have a pre-F_1 fabric which can be attributed to a low-grade metamorphism (Appendix 1, thin section 5). Therefore, only one phase of retrogression of the basement lithologies is assumed within the area studied.

3.2 F_1 Tectonothermal Microstructure

The textural changes associated with the sericitization and quartz recrystallization are very similar in the basement and cover lithologies. Talbot (1964) described the process of phyllonitization in the Houghton Complex and adjacent Torrens Group lithologies. Within the basement, a gradational change from medium to coarse grained, subgranoblastic gneisses and schists to finer augen schists, is a result of the development of recrystallized quartz and sericite aggregates in bands around relict quartz/feldspar lenticles and pods (Appendix 1, thin sections 6-11).

Talbot, Davies and McEwin consider that the phyllonitization may be related to zones of shearing in the basement adjacent to the basement-cover contact on the overturned linb. The increasingly sheared nature of the outcrop is related to greater degrees of sericitization, quartz recrystallization and fracturing of feldspar grains. A corresponding alteration of brown biotite to green biotite and then to chlorite or opaque oxides occurs across a well defined zone within the basement adjacent to the west limb. The resulting lithology in the centre of this zone is a green, chlorite and sericite, mylonitic, quartz augen schist which contains a high degree of quartz and feldspar recrystallization. This rock type is comparable with the mylonitic "Oystershell Rock" described in the Moine Thrust Zone (Barber and Soper, 1973). A similar zone of irregularly foliated, chloritic schist occurs in the Tapley Hill Formation on the east limb (Plate 1) and may also represent a zone of more intense deformation.

Paralleling the decrease in phyllonitization, the increase of biotite into less deformed lithologies on either side of the basement chlorite zone, results in a light grey to light brown, biotite, sericite, augen schist with chlorite either very minor or absent (Appendix 1, thin sections 8-9). This lithology is most widespread and often contains

pegmatites which crosscut and parallel the foliation, suggesting they are syn-tectonic with the phyllonitization. These pegmatites may be syngenetic with thin stringers of quartz/feldspar segregations in the basal cover units which are adjacent to the basement-cover contact, particularly in the regional fold nose.

The progression from granoblastic gneissic schists to the phyllonitized, mylonitic schists is not regular in the basement; pods of unphyllonitized basement occur within the mylonitic schists. However the trends of phyllonitization and chloritization are approximately planar and are parallel to the lower basement-cover contact (Plate 1). These planar zones of localized strain states with well developed LS fabrics are described as shear zones by Ramsay and Graham (1970). Therefore a ductile shearing deformation associated with the phyllonitization may be contemporaneous with, or postdate the F_1 fold formation. In the zones of intense shearing, the retrogressed basement lithologies which remain after regional F_1 greenschist metamorphism, are further retrogressed by alteration of the relict feldspars to sericite and biotite to chlorite. The lower degree of phyllonitization and biotite alteration in the cover lithologies reflects the less intense shearing and fabric development.

3.3 Nature of the Deformation Associated with the Fabric Formation

Talbot (op.cit.) assigned the name blastomylonites to the recrystallized sheared rocks. However this term implies intense cataclastic deformation prior to the recrystallization (Christie, 1960). The deformation appears to have proceeded by the ductile deformation processes of mylonite formation described by Bell and Etheridge (1973), although there is some cataclastic fracturing of the deformed quartz relicts, and more commonly, of the feldspars. These fractures generally occur at an angle greater than 45 degrees to the foliation and are infilled by sericite and fine recrystallized quartz. With increasing

phyllonitization, the quartz schists become more elongate and xenoblastic. A high degree of undulose extinction and deformation band development suggests ductile intracrystalline slip is the major process of deformation.

The subgrain development and quartz recrystallization commonly occurs around the relict quartz margins and along planar zones within the grains. They are the result of a recovery process in response to the P.T. conditions imposed by the ductile deformation. The high degree of recrystallization suggests that high temperatures existed during the late stages of the deformation (Williams, 1975). The pressure shadow development due to recrystallization is minor, and therefore, the coarse recrystallized quartz grains in the basal cover units exhibit the shapes of subellipsoidal elongated original grains (Appendix 1, thin sections 1-2).

4. RELATIONSHIP OF FABRICS TO DEFORMATION

4.1 Foliation

The slaty cleavage in the metasilts and the irregular foliation in the more massive cover sediments parallel the foliation developed in the basement (Plate 2). All are genetically related as the axial plane foliation of the regional fold, although the foliations related to high degrees of phyllonitization are possibly related to shearing movements related to the overturned limb.

Where there is a very intense foliation developed in the cover units, the short limbs of the large-scale mesoscopic folds are often sheared out and discontinuities in the units occur between the consecutive long limbs. These breaks in cover lithologies are readily observable in the prominent basal conglomerate and Sturt Tillite on the overturned limb.

4.2 Lineations

Persistent lineations throughout the area may be subdivided into two groups; those which reflect fold geometry, and alternatively, lineations which are genetically related to the development of an elongation lineation. Clastic grain or pebble elongation and mineral streaking in the cover lithologies, in addition to mineral streaking of mica grains in the basement lithologies, are placed in the first group. In contrast, cleavage-bedding intersections and fold axes are elements of the folding.

All these lineations are sub-parallel with a constant shallow plunge to the southeast, approximately orientated downdip within the foliation planes.

4.3 Macroscopic Variation in Fabric Orientation

Contours of the elongation lineation plunge trajectories are shown on the reconstructed pre-thrusting map (Figure 3). Within

the basement, the lineation plunge varies systematically, with zones of low angle (e.g. 20 degrees) plunge paralleling the overturned limb and approximately corresponding with the zones of high phyllonitization and mylonitization. These planar zones which occur adjacent to the basement-cover contact of the west limb of the Myponga-Little Gorge Inlier, are collectively named the Anacotilla Shear Zone, after the Anacotilla River which flows along the zone near the nose of the regional reclined fold.

A southeast-northwest vertical cross-section across the shallow plunge zone at location 3 (Figure 3), is shown in figure 4A. From northwest to southeast, the variation from high angle fabric plunges of approximately 55 degrees to low angle plunges of 15 degrees then steepening again, corresponds with the increase of the sheared nature of lithologies towards the basement cover contact. The shallowest plunge occurs in the highly chloritic mylonite adjacent to the contact. Steep foliation and lineation plunges correspond with relatively unsheared dolomitic sandstones and granoblastic gneissic schists at either end of the cross-section.

4.4 Nature and Orientation of the Simple Shear Model

The systematic variation of the fabric orientation and its association with the degree of phyllonitization, suggests that both the lineation and foliation development in the basement are related to a simple shear mechanism. This possibly implies plane strain conditions during shearing.

The orientation of the simple shear zone implied by the fabric variation across the section shown in figure 4A, is estimated by assuming the initial angle (θ') of fabric development is orientated at a maximum of 45 degrees to the shear direction (Ramsay and Graham, 1970). Therefore the steepest foliation dip of 55 degrees to the east, orientates the walls of the shear zone as dipping approximately

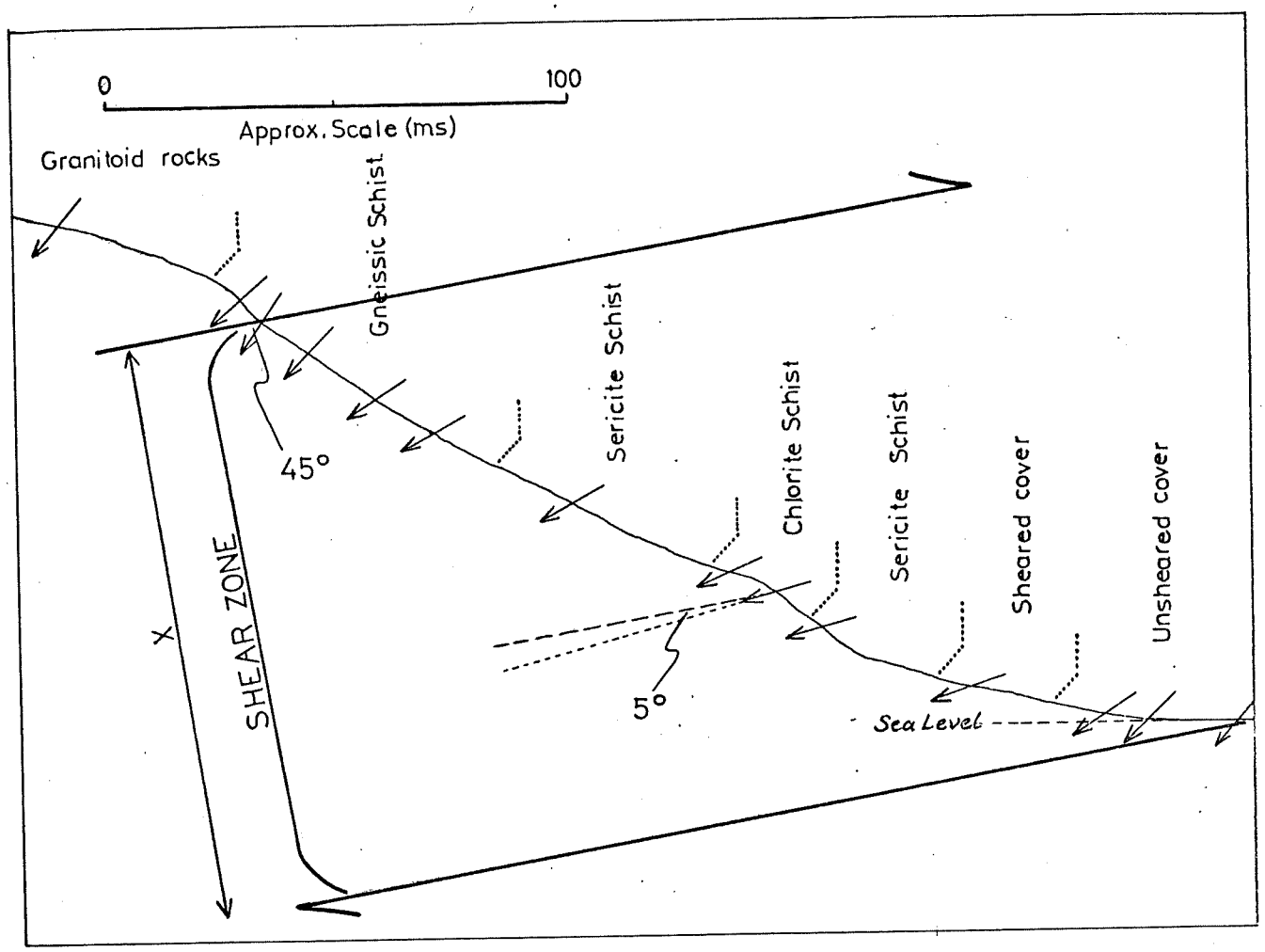

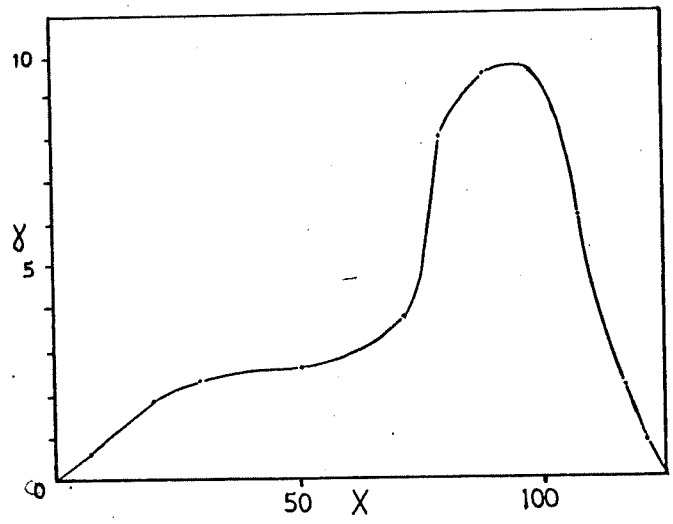

FIGURE 4. A. MODEL OF SIMPLE SHEAR ZONE. *True vertical section at location 3, looking southwest. Profile of water course drawn from a photograph. Vertical scale is not exaggerated. Small arrows represent fabric dips. Large arrows represent the shear zone walls and direction of movement.*

B. VARIATION OF SHEAR STRAIN ACROSS THE SHEAR ZONE. *Scale of the X axis is the same as for A. Area under the profile represents a total displacement of .5 km. across the shear zone.*

10 degrees to the southeast in true cross-section. Hence the minimum foliation dip of 15 degrees is orientated 5 degrees to the shear direction (i.e. θ'=5 degrees). As the shear strain (γ) is determined by tan $2\theta'$ = $2/\gamma$ (Ramsay and Graham (op.cit.)), the maximum value of γ within the shear zone is approximately 10.0. The variation of γ across the shear zone is shown in figure 4B. As the relative movement on either side of the shear zone is estimated by calculating the area under the profile of γ versus perpendicular distance across the shear zone (x), figure 4B indicates a movement of 500 metres of the upper wall of the shear zone over the lower.

The orientation of the shear zone is expected to parallel the overturned basement-cover contact, therefore an estimated dip of 10 degrees for the shear direction may be too shallow. If the initial fabric orientation is less than 45 degrees to the shear direction, the maximum shear strain is higher and the shear zone dips more steeply to the southeast in closer parallelism with the west limb. The distance of overthrusting would be greater.

Another alternative, is that the axial plane foliation was sufficiently developed prior to the shearing, so that a pre-existing foliation is reorientated within the shear zone. The γ value calculated above would be invalid if this were the case.

5. STRAIN ANALYSIS OF PEBBLES AND QUARTZ GRAINS

5.1 Nature of the Basal Conglomeratic Arkosic Sandstone

The basal conglomerate and arkosic sandstone provide the most suitable markers for the estimation of finite strains. Both the distinctive character and persistence of the unit and its stratigraphic position adjacent to the cover-basement contact permit ready determination of sample locations relative to the contact and the regional fold. Variability of mechanical behaviour during deformation due to lithological differences, is low due to the homogeneity of the unit throughout the area. Bedding orientations are readily determined by the ilmenite layering, which is still fine enough for the sandstone to retain an overall homogeneity.

The nature of the outcrop of this hard homogeneous unit is one of angular jointed blocks, which often provide excellent planar surfaces sub-parallel to the principal planes of the local strain ellipsoid (Photographs 1-2).

Microscopic examination of 38 slides of the arkosic sandstone reveals a consistent initial sedimentary composition (Appendix 2). The concentration of clastic grains in comparison with the fine grained matrix, varies from 65-90 percent, whereas the detrital quartz and feldspar percentages are 45-70 and 10-25 percent of the total rock respectively. The average grain size of the detrital grains vary from 1 to 2 millimetres only. Detrital ilmenite constitutes 1 to 4 percent of the rock.

Deformation of the arkosic sandstone has resulted in the predominantly ductile deformation of the quartz grains by intracrystalline slip and has also resulted in the development of a foliation by lepidioblastic sericite growth. The quartz grains are flattened in the cleavage plane and show moderate to high degrees of undulose extinction and deformation band development (Carter, Christie and

Griggs, 1964).

Between 20 and 100 percent of the detrital quartz is recrystallized. Polygonal subgrains and unstrained recrystallized grains of fine, uniform grainsize (.05-.3 mm) are distinct from the coarse and highly undulose xenoblastic relict quartz grains. Experimental observations indicate that a recrystallized aggregate occupies a smaller volume than the original strained grains (Williams, 1975). However the volume change is not considered significant enough to produce an apparent volume change due to deformation processes. An apparent oblate strain due to recrystallization is, therefore, not expected (Ramsay, 1967).

There is no exact relationship between the degrees of quartz recrystallization and amount of sericitization in the sandstone. However the amount of recrystallization increases in an approximately linear manner with the intensity of the ductile deformation of the quartz grains (Appendix 2 cf. Table 1). Therefore, there appears to be a direct relationship between the degree of recovery and the amount of ductile strain the sandstone has undergone. In contrast, experimental observations indicate that high degrees of recrystallization reflect high temperatures and low deformation (Williams, 1975). Experimentally, the recrystallized grainsize reflects the degree of deformation, however the recrystallized quartz grainsize is uniform throughout the arkosic sandstone.

The contrasting ductilities of the detrital quartz and feldspar grains necessitates the measurement of quartz grains only as consistent strain markers. The ductility contrast between the quartz grains and the feldspar/sericite matrix may produce a rotational couple and complex grain strains. In comparison, the feldspathic quartzite pebbles in the conglomerate are similar in nature to the arkosic sandstone matrix. To maintain a constant strain marker

ductility, the highly feldspathic granitoid pebbles present in the conglomerate, were not measured.

5.2 Methods of Measurement

Subellipsoidal pebble and quartz grain strain markers were measured on approximate principal planes of the local strain ellipse. Pebble measurements were made on planar joint surfaces in the field and from photographs, whereas grain shape measurements were measured from thin sections cut parallel to the appropriate principle planes.

In most cases, planes parallel to the XZ and YZ principal planes were measured at each location. Joint surfaces with measurable XY pebble forms were difficult to find in the field. Also, for oblate strains, the X orientation may be difficult to determine on the XY plane, whereas the extremities of the particles in the X direction are often difficult to locate for high strains (Dunnet, 1969). The principal directions are readily determined on both the scales of outcrop and hand specimen, by the orientations of the elongation lineation (X) and the cleavage plane (XZ). No corrections were necessary for the orientations of the planes of measurement as all the surfaces used were within 10 degrees, and most within 5 degrees of the principal strain planes. The thin sections were projected through a standard slide projector normally onto a screen from which grain outlines were traced. This method of measurement produced negligible distortion of the grain shape ratios and orientations.

Between 45 and 70 quartz grains were measured for each thin section, whereas 35 to 55 pebbles were measured on each joint surface examined. A total number greater than 50 for each section is desirable, as 50 to 60 measurements is considered to be a minimum statistical sample (Dunnet, 1969).

Impinging grains and pebbles were not measured due to strain inhomogeneity at the interacting grain or pebble boundaries. A micro-

scopic examination of each thin section under crossed polars, was made prior to strain measurement. The mineralogical and microstructural characteristics of each sample were determined and brittle feldspar grains were distinguished from the detrital quartz outlines. However the distinction is not absolute, resulting in slightly lowered average quartz grain ratios. A random measurement of quartz and feldspar grains in one thin section produced a decrease of the estimated logmean axial ratio of 6 percent. As the same quartz/feldspar discrimination technique applies to all sandstone samples, a similar small reduction is assumed for every logmean axial ratio estimate.

5.3 Rf/Ø Diagram Analysis

"Strane", a FORTRAN IV program developed by Dunnet and Siddans (1971), is an extension of the graphical Rf/Ø diagram analysis technique developed by Dunnet (1969). The program is used to estimate the tectonic strains that are superimposed on initial sedimentary fabrics or earlier deformational strains.

For a principal plane, the relationships of the axial ratio (Rf) and the long axis orientation (Ø) of each grain with respect to the orientations of the cleavage and bedding traces in that plane, are considered. During irrotational pure shear, the rate of rotation of the bedding trace towards the cleavage trace, will be less than that of the long axis of an elliptical grain as the former is a material line of the rock being deformed, whereas the long axis is only a geometrical property of the grain. Gay (1968a) derived the relation which represents the deformation path on the Rf/Ø graph, of an elliptical particle in a rock of homogeneous ductility, which is undergoing a pure shear deformation. Subsequently, Dunnet (op.cit.) derived a set of curves which relate the finite strain (Rs) which has been applied to an initial axial ratio (Ri) for an originally random fabric. Rs and Ri are determined by the fit of a suite of Rf and Ø plots to Dunnet's

calculated curves.

Dunnet and Siddans (op.cit.) extended the graphical Rs and Ri analysis technique to non-random planar and semi-planar initial (Rs=0) fabrics. For such fabrics, the Ri values for a statistical suite of particles are not random in relation to the Θ (long axis orientation in initial fabric) values. Instead, the Rf/$\emptyset$ values have a symmetrical distribution about the bedding trace, logmean Ri and mean Θ. "Strane" calculates the Rf and $\emptyset$ values for each ellipse in the principal plane from the long and short axes measurements and from the difference between the orientations of the long axes and the X principal direction. Logmean Rf and mean $\emptyset$ are determined. "Strane" then removes successive increments ($.1\bar{\varepsilon}$) of pure shear strain from each Rf/$\emptyset$ point, which are, therefore, translated along the deformation path until the suite of Rf/$\emptyset$ points is symmetric about the bedding trace or about mean $\emptyset$. In this situation the Rf and $\emptyset$ values are considered to be the Ri and Θ values of the initial fabric. Rs is determined by the total number of unstraining increments at maximized symmetry.

5.4 Suitability of Rf/$\emptyset$ Diagram Analysis

Two assumptions are made in using Rf/$\emptyset$ diagram analysis to determine Rs and Ri.

(a) It is assumed that the deformation is an irrotational pure shear. Throughout the area studied, the fabric variation suggests a simple shear mechanism is associated with the deformation. Therefore the intensity of the deformation is related to the rotation of the principal strain axes within the shear zone. The maximum rotation of the X axis between the lowest and most highly deformed lithologies is possibly 40 degrees. However the majority of the elongation lineations measured have moderate plunges and therefore, have moderate angles with the shear direction. Consequently, the rotational component

of the simple shear can be considered minor and the deformation associated with the pebble and quartz grain strains is an approximate irrotational pure shear.

(b) The second assumption of zero ductibility contrast between the particles and matrix is valid in consideration of the small compositional difference between the pebbles and the sandstone matrix in the conglomerate. Similarly the high (50-70 percent) total rock concentration of the detrital quartz grains in the arkosic sandstone, suggests that a reduced viscosity ratio is to be expected (Gay, 1968a). Therefore the rotational couple acting on the quartz grains due to viscosity ratios is expected to be low.

5.5 Results of Rf/Ø Diagram Strain Analysis

Two, or in some cases three, principal planes of 19 arkosic sandstone samples and 7 conglomerate samples have been analyzed by "Strane". The results are listed in Table 1.

The Ri values obtained by mathematically unstraining the deformed rock to a possible initial fabric, are low for both the pebbles and quartz grains. For the quartz grains, the suggested initial X/Z and Y/Z ratios are 1.69±.44 and 1.59±.31 respectively. These values indicate subspherical to slightly oblate grain shapes, which may be representative of initial sedimentary fabrics. The corresponding Rs values are variable, reflecting different magnitudes of strain which are superimposed on the initial fabric. As expected, the X/Z Rs values are greater than Y/Z values.

Alternatively, Rs and Ri values are determined by the fit of the suites of the Rf/Ø suites to Dunnet's standard curves. In most cases, the Rf/Ø suites are symmetrical with respect to the Ø=0 trace for the arkosic sandstone, suggesting a random initial fabric (Figure 5,A). In comparison, some faces have a non-symmetrical distribution with a greater concentration of points near the bedding trace

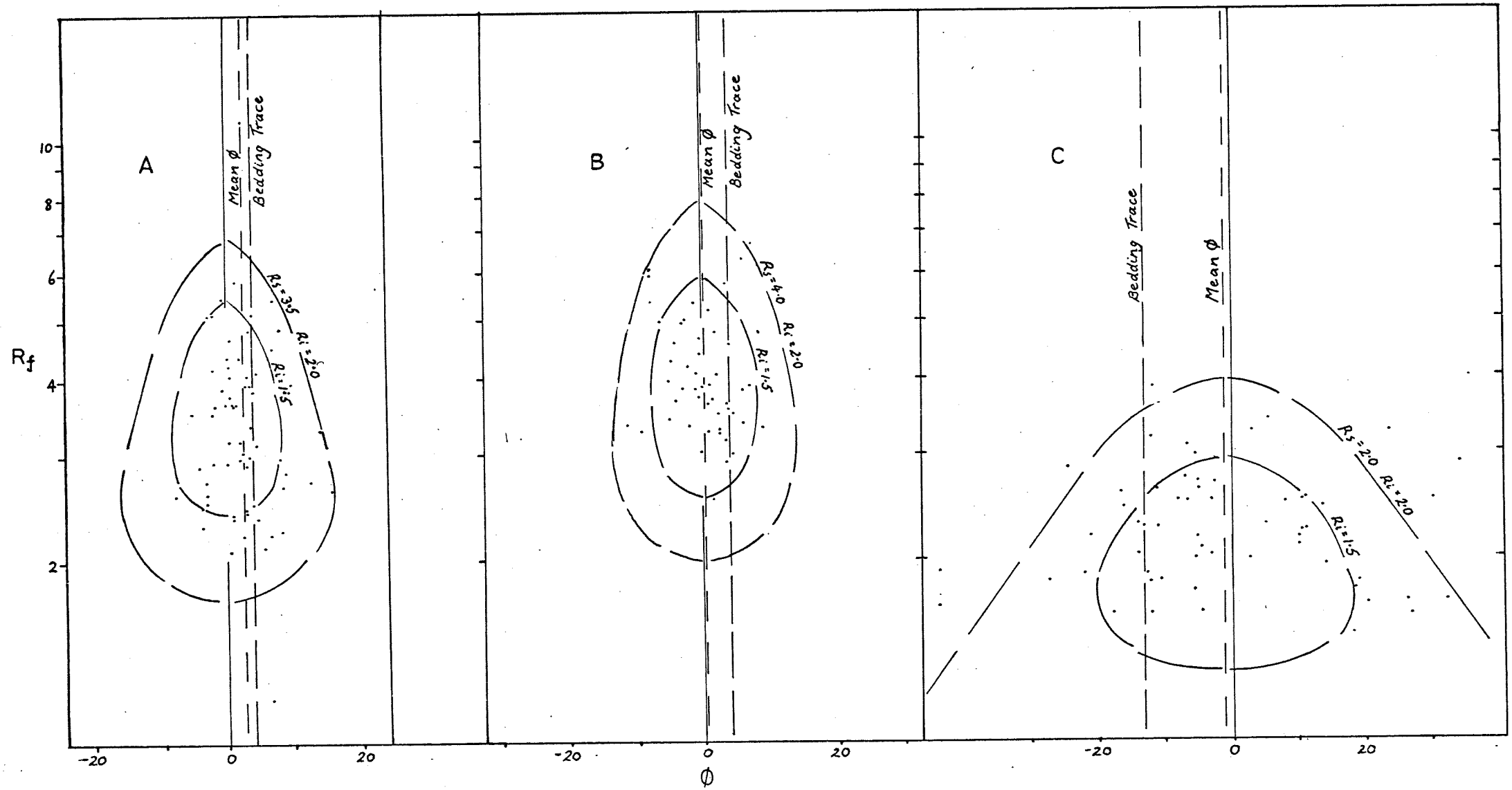

FIGURE 5. R_f/ϕ DIAGRAMS

A. Sample 455/G2, YZ principal plane. Suite of points is approximately symmetrical about the cleavage trace, representing a highly random initial fabric.

B and C. Sample 455/16C17, XZ and YZ principal planes respectively. Best fitting standard Rf/ϕ curves have similar Ri values in contrast to the higher Rs values for the XZ plane. The concentration of points near the bedding trace suggests an initial planar sedimentary fabric.

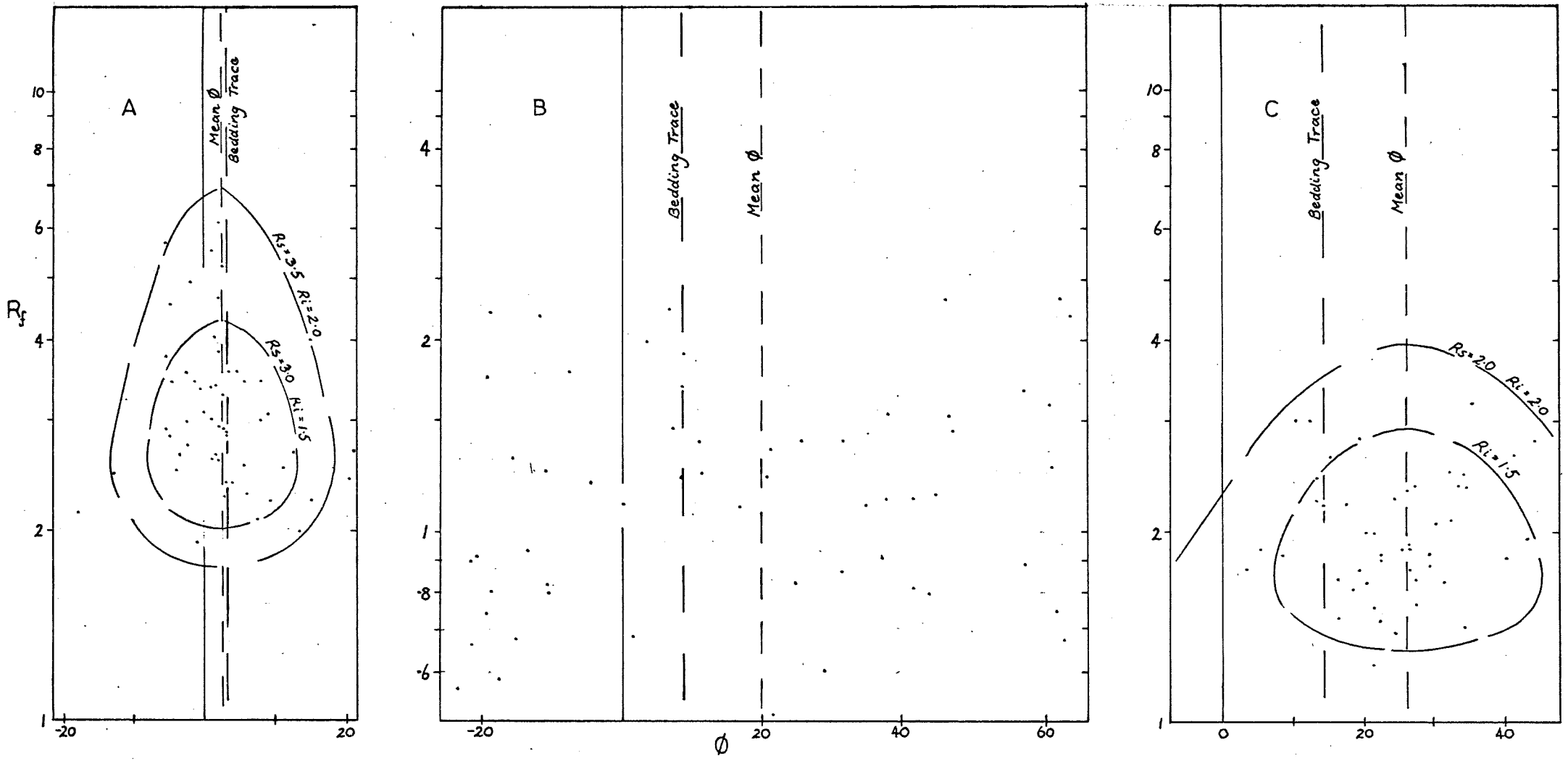

FIGURE 6. R_f/ϕ DIAGRAMS

A and B. *Sample 455/A1, XZ principal plane. Example of a deformed semi-planar fabric. A, Rf/Ø diagram with best fit standard curves; B, reconstructed diagram after removal of a strain ratio of 2·8:1. The distribution of points is symmetric w.r.t. mean Θ. Logmean Ri is 1·13 and Θ ranges from -24 to 64 degrees.*

C. *Sample 455/C CONG, YZ principal plane. Example of a weakly deformed conglomerate with an initial sedimentary imbricate fabric. Pebbles have a preferred orientation about mean Ø which is steeper than the bedding w.r.t. the cleavage trace.*

(Figure 5,C). Therefore an initial non-random planar or semi-planar fabric may have existed. Quartz grain Ri values determined by Dunnet curves are 1.45±.16 and 1.57±.14 for the XZ and YZ faces respectively.

The XZ principal plane of sample 19 (Appendix 2) has an approximate symmetrical Rf/Ø distribution about the Ø=0 axis due to the near parallelism of the bedding trace with the axis (Figure 6,A). Unstraining of the grains by "Strane" results in a symmetric distribution around mean Ø when Rs = 2.8 and Ri = 1.13 (Figure 6,B), which agree with the estimated Dunnet curve values of Rs = 3.0 and Ri = 1.0 - 2.0. The Ri/Θ plot is representative of a semi-planar initial fabric. Although the angle between mean Ø and the bedding trace is 12.5 degrees, the low Ri values and lack of concentration of the points about mean Ø do not support a true imbricate fabric.

Rf/Ø diagrams of the conglomerate pebbles reveal more imbricate fabrics. Sample 20 YZ (Figure 6,C) has undergone little deformation (Rs = 1.5-2.0) and therefore shows an approximate original fabric on the Rf/Ø diagram, which shows a symmetrical distribution of points about mean Ø which intercepts the bedding trace at angle of 11.5 degrees.

Assuming that sedimentary imbricate fabrics dip upstream, the orientation of the initial pebble fabrics may be used as palaeocurrent indicators. The regional fold axis is rotated within the axial plane to a position of zero plunge, which corresponds with the shallow plunges of the equivalent F_1 regional folds on the southeastern side of Fleurieu Peninsula (Daily and Milnes, 1973). The fold is then unfolded to an initial horizontal deposition surface (Figure 7).

If the angle between mean Ø and the bedding trace is less than 5 degrees, the fabric is considered to be planar, which is the situation for the majority of pebble faces. In the reorientated, unfolded position, two YZ pebble faces have an imbrication dip to the

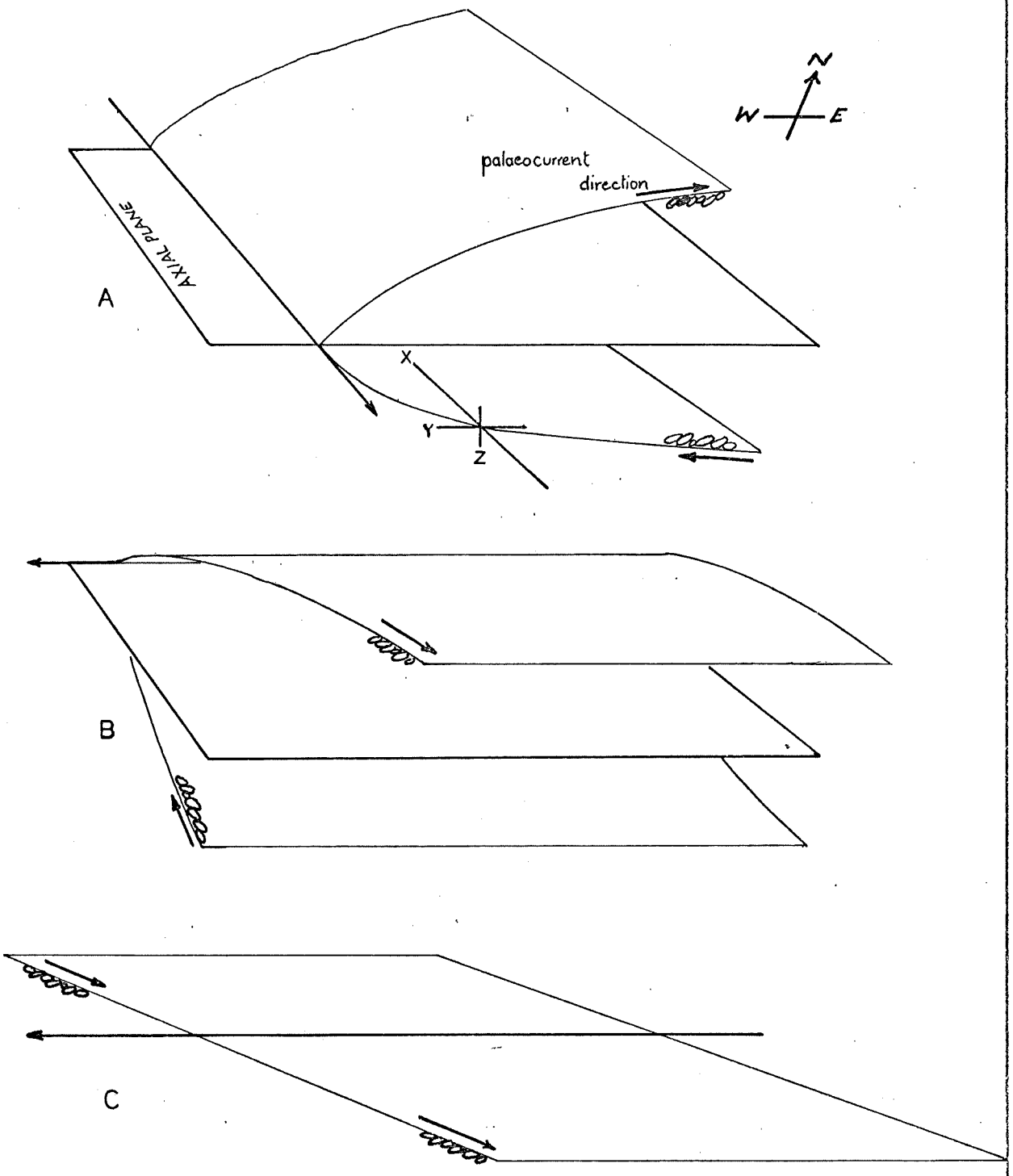

FIGURE 7. UNFOLDING OF THE REGIONAL FOLD

Imbricate sedimentary fabrics determined by Rf/ϕ analysis for the YZ principal plane, suggest northwest palaeocurrents, if the fold is unrotated as above.
A to B involves rotation of the fold axis within the axial plane. B to C requires the rotation of the limbs about the fold axis to a horizontal deposition plane.

northwest. No other imbricate fabrics are recognized. Although this only suggests a northwesterly palaeocurrent component, it is in agreement with either a general flow from the western Stuart Shelf, which is believed to be a high in Torrensian times (Parkin, 1969) or a north-south current flow along the axis of the Adelaide Geosyncline.

5.6 $\bar{E}s$ and V Estimates

The logmean of the axial ratios measured in each of two principal planes per locality of assumed homogeneous strain, were combined to give three axial ratios. On reducing the Z axis to unity, the X and Y ratios are placed in the program "Gnam" (James, 1975), which calculates the natural logarithmic strain ($\bar{E}s$), Lodes Unit (V), the shortening parallel to Z (across the cleavage), the shortening parallel to Y and the elongation parallel to X. $\bar{E}s$ is directly proportional to the natural octahedral unit shear, which is an absolute measure of the magnitude of the distortional component of strain of any symmetry (Hossack, 1968). V is a measure of the symmetry of finite strains and is analogous to Flinn's k. For simple extension $V = -1.0$ ($k = \infty$), plane strain $V = 0.0$ ($k = 1.0$) and simple compression $V = +1.0$ ($k = 0.0$).

$\bar{E}s/V$ plots on the natural strain plane of the pebble (crosses) and quartz grain (dots) strains are shown in figure 8A. The numbers refer to the location of each sample which are plotted on plate 1. All points plotted are $\bar{E}s/V$ calculations from XZ and YZ logmean Rf values, excepting sample 5 which represents pebble strains calculated from XY and YZ measurements.

All three principal planes were measured for pebble sample 2 and quartz grain sample 7. Consequently three $\bar{E}s$ and V estimates are possible for either sample by the three combinations of two of either the $^{X}/_{Y}$, $^{Y}/_{Z}$ or $^{X}/_{Z}$ ratios. The two opposite vertices of the triangles associated with points 2 and 7 are XZ:XY and XY:YZ Es and V estimates.

TABLE 1: RESULTS OF STRAIN ANALYSIS

QUARTZ GRAINS

Field No.	Location	Face	No. ellipses	Log-mean Rf	Rf/Ø Analysis		Es	V
					Rs	Ri		
455/2C6	1	XZ YZ	65 64	4.85 2.83	- -	- -	1.14	.32
455/3C11	3	XZ YZ	60 66	5.70 3.24	3.6	1.78	1.26	.35
455/7C1	6	XZ YZ	55 51	3.01 2.82	2.2 1.7	1.19 1.80	.87	.88
8C2	7	XZ YZ XY	60 50 60	3.68 2.50 3.29	2.2 1.4 -	1.80 1.79 -	.95 1.49 1.02	.41 -.13 -.83
NC2	9	XZ YZ	56 57	4.85 2.10	2.5 1.1	2.21 1.94	1.12	-.06
NC3	10	XZ YZ	50 50	7.36 2.87	- 2.2	- 1.30	1.41	.06
M3	11	XZ YZ	62 60	2.56 2.06	- 2.1	- 1.16	.70	.54
M6	12	XZ YZ	55 55	2.81 2.64	2.9 -	1.70 -	.82	.88
I1	13	XZ YZ	55 55	3.44 2.50	2.5 2.1	1.42 1.24	.91	.48
G4	14	XZ YZ	60 63	4.75 2.33	- 3.0	- 1.44	1.10	.09
G1	15	XZ YZ	55 61	6.80 3.33	6.1 -	1.16 -	1.37	.26
G2	16	XZ YZ	62 65	10.90 3.35	- -	- -	1.69	.01
E1	17	XZ YZ	60 64	3.87 2.21	- -	- -	.96	.17
A1	19	XZ YZ	55 60	3.07 2.19	2.8 1.2	1.13 1.87	.81	.40
16C17	21	XZ YZ	50 58	4.03 2.23	3.5 3.8	1.16 1.12	.99	.15
17C7	23	XZ YZ	50 55	5.27 2.00	- 1.3	- 1.6	1.18	-.17
17C8	24	XZ YZ	60 57	5.26 2.21	2.6 1.9	2.15 1.57	1.17	-.04
17C10	25	XZ YZ	62 60	4.94 2.27	3.3 -	1.5 -	1.13	.03
20C1	26	XZ YZ	55 50	3.39 2.45	- 3.0	- 1.11	.89	.47

TABLE 1: RESULTS OF STRAIN ANALYSIS (cont'd)

CONGLOMERATE PEBBLES

Field No.	Location	Face	No. ellipses	Log-mean Rf	Rf/Ø Analysis		Es	V
					Rs	Ri		
455/2CONG	2	XZ YZ XY	45 51 35	7.35 2.33 4.94	- 1.9 -	- 1.33 -	1.49 1.42 1.75	-.6 -.15 -.31
3CONG	4	XZ YZ	45 63	5.55 2.37	- 1.7	- 1.42	1.21	.0
7CONG	5	YZ XY	50 40	2.01 10.32	1.6 -	1.28 -	1.69	-.4
T CONG	8	XZ YZ	51 50	3.92 2.94	- -	- -	1.02	.58
D CONG	18	XZ YZ	45 45	5.35 3.10	- 2.6	- 1.24	1.21	.35
C CONG	20	XZ YZ	45 50	4.99 1.95	1.3	1.74	1.14	-.17
16 CONG	22	XZ YZ	15 30	3.87 2.28	- -	- -	.96	.22

The large error triangle associated with the sandstone sample 7 is largely due to a misorientated XY thin section cut. However the error suggested by the triangle associated with the conglomerate sample is considered more typical of the errors of the $\bar{E}s/V$ estimates. This error is believed to be largely due to the preferred orientation of axes outside the principal planes as well as the greater errors which arise from measurements on the XY plane mentioned earlier.

5.7 Variation in the Finite Strains

The $\bar{E}s/V$ plots shown in figure 8A are considered to be a good representation of the finite strain variations for the pebble and quartz grain shape ratios. If a similar error triangle applied to point 5 as that of point 2, then the equivalent XZ:YZ estimate for sample 5 may occur in the vicinity of point 5'.

Es/V values of both pebbles and quartz grains from various locations, plot in the same trend of increasing prolateness with increasing magnitude of the distortional component of strain. The lowest strains in the area are highly oblate (V = .55 - .90) whereas V values of 0.0 to -.2 correspond to the highest $\bar{E}s$ values. The trend of the possible deformation path is a straight line (Figure 8) representing a deformation of the type $a = b^k$ by Flinn's (1965) notation.

The change in symmetry with increasing strain possibly indicates a prolate progressive strain is superimposed on an initial strain of $\bar{E}s$ = .70-.95 and V = .5 - .9. As these values suggest initial axial ratios of approximately 3:2.5:1, it is unlikely that the prolate strain is superimposed on a sedimentary fabric with detrital quartz grains of such oblateness. Although highly oblate sedimentary quartzite pebbles are possible, the parallelism of the pebble and quartz grain finite strain variation suggests a non-sedimentary fabric existed prior to the prolate strain.

Therefore a weak flattening and foliation development

A.

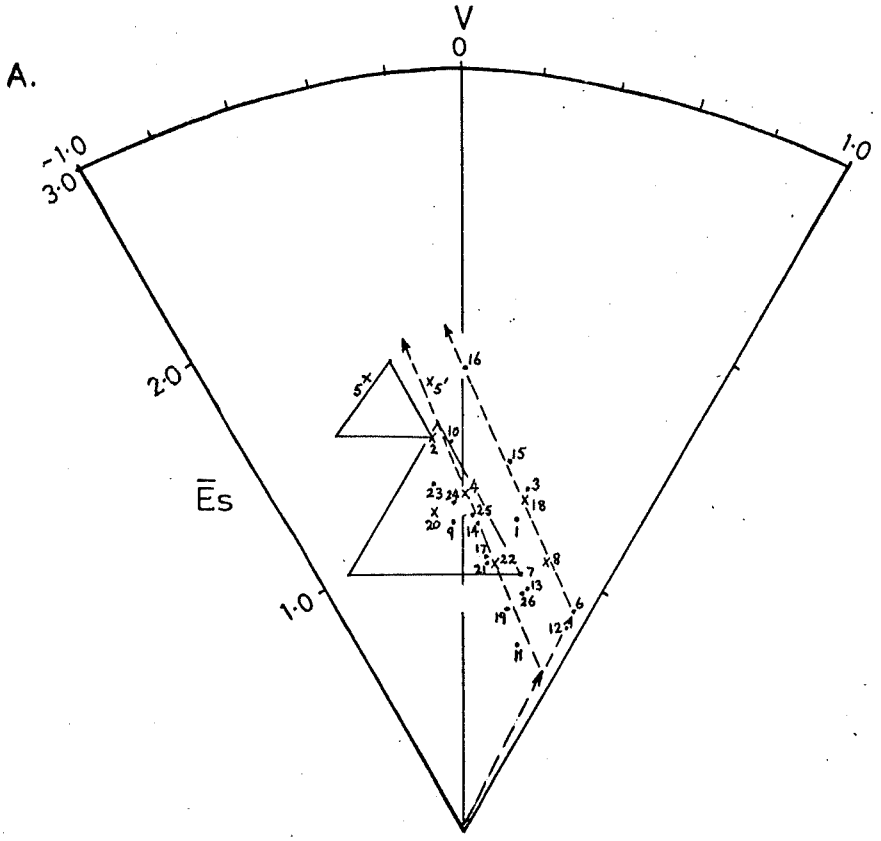

B.

FIGURE 8. VARIATION OF FINITE STRAIN ESTIMATES

A. *Plot of* $\bar{E}s/V$ *values showing variation of estimated natural finite strains. Arrowed dashed lines are possible deformation paths. Triangles represent errors as discussed in the text.*

B. *Photograph of thrust slice of east limb conglomerate unconformably overlying basement. Cover lithologies - C ; basement lithologies - B. Heavy dashed lines - thrusts ; light dashed line - unconformity. West limb cover units occur in distant left. Facing northeast at the Congeratinga River mouth. Numbers refer to sample locations. By comparison with A, a progressive increase in* $\bar{E}s$ *and decrease in V across the thrust slice is apparent for locations 13 - 16.*

associated with the deformation which produced the regional F_1 folding, may have preceded a prolate strain development. The oblate strain values indicate a shortening parallel to Z of nearly 50 percent which may be sufficient to produce the strong foliation and slaty cleavage observed. Cloos (1947) estimated only 30 percent flattening is necessary to produce a slaty cleavage in calcareous units.

The Ri values determined from "Strane" and graphical Rf/Ø diagram analysis are commonly less than 1.5:1.5:1 and rarely greater than 2:2:1 for the quartz grains. These values are most likely to be realistic estimates of the sedimentary grain axial ratios and therefore, the Rs values determined by Rf/Ø diagram analysis represent the superimposed strains of both the folding and later prolate strain deformations. In view of the low Ri values, the Rs values are expected to be approximately equivalent on slightly less than the measured Rf values. A comparison of the Rf and Rs values verifies this (Table 1).

Although expected, Rf/Ø diagram analysis does not reveal an initial planar fabric which parallels the cleavage prior to the proposed prolate strain deformation. The reason is not apparent, but where initial non-random sedimentary fabrics may have existed, the low magnitude of the oblate strain would not have produced a planar fabric about the foliation. Alternatively, the principal axes of the two superimposed strains may not have been parallel, in which case the fabric which resulted from the oblate strain, would not be planar to the XY plane of the later prolate strain.

5.8 Regional Distribution of Strains

The reconstructed map of the regional fold (Figure 9) shows the aerial distribution of the $\bar{E}s$ and V values prior to the brittle faulting. Only the lateral component of the two major thrusts is re-

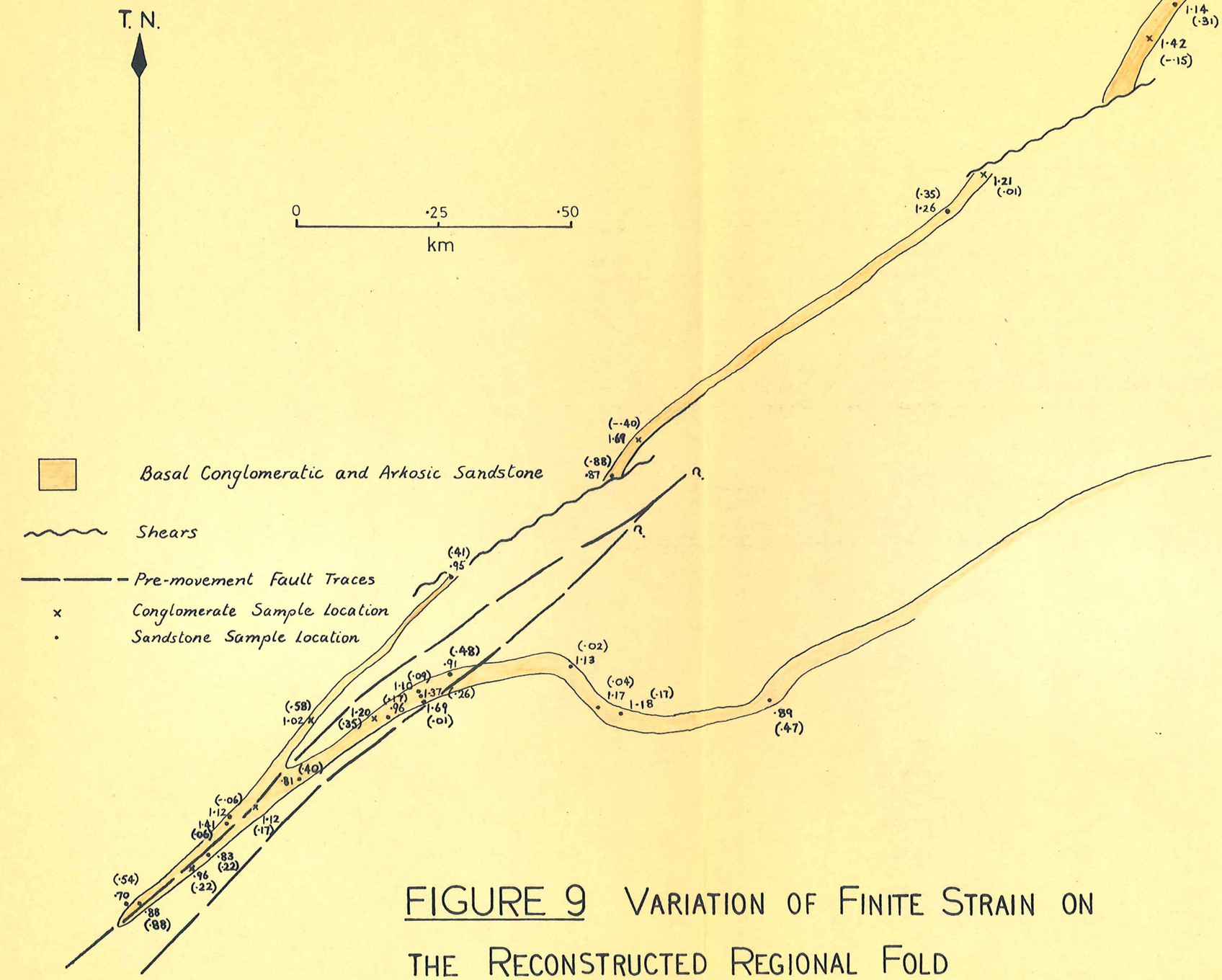

FIGURE 9 VARIATION OF FINITE STRAIN ON THE RECONSTRUCTED REGIONAL FOLD

$\bar{E}s$ values stated at each location.

V values in brackets.

moved to produce a closure in the fold nose. Although the strain components are difficult to contour, the values are progressive within the original thrust slices and are continuous across the trace of the thrusts. A homogeneous area of low $\bar{E}s$ values occurs in the reconstructed fold nose. This suggests that the magnitudes of strain arising from the fold formation are low. A progressive increase in $\bar{E}s$ from northwest to southeast across the central thrust slice occurs for samples 14, 15 and 16 (Figure 8B).

There is a good correspondence of $\bar{E}s$ and V estimates across the reconstructed fault planes. In the fold nose, there is an agreement of values across the lower fault whereas the plane strain values of samples 23-25 correspond with the progressive decrease of V toward the upper thrust in the east limb.

Sandstone samples taken near conglomerate sample locations generally have approximately equal or lower Es and correspondingly, more oblate V values. The difference may be a result of the different ductilities of the quartz grains and quartzite pebbles. The pebbles are deforming with a higher strain rate due to a greater ductility than the quartz grains.

5.9 Discussion of Strain Results

The apparent deformation paths delineated by the finite strain variation within the conglomerate, suggest that a prolate strain has developed from a low magnitude oblate strain, which is associated with the regional axial plane foliation developed during folding. This implies that the elongation lineation post-dates the regional fold formation.

However the development of the LS fabric in the planar zones of intense deformation, is considered contemporaneous with the formation of the elongation lineation. Therefore the prolate and oblate finite strains appear to be generated by a simple shear mechanism, where-

by a plane strain is superimposed on an oblate strain. For this to occur, the X axes of the oblate and plane strain ellipsoid must have the same orientation, whereas the Y and Z axes of the successive deformations are interchanged (Figure 10). If the XY plane of the initial oblate strain is the axial plane of the regional fold, then the XY plane of the superimposed plane strain is perpendicular to the axial plane if the resulting finite strain is to be prolate. This situation cannot apply to the area studied as the LS fabric developed in the zones of intense deformation is sub-parallel to the axial plane of the fold. Hence the XY plane of the strain ellipsoid which is associated with the proposed simple shear, is sub-parallel to the XY plane of the strain ellipsoid related to the fold formation.

If the major deformation mechanism is considered to be simple shear from which plane strain results, then the estimated prolate finite strains are anomalous. This problem may be explained in two ways:

(a) The first possibility is that the inferred deformation paths may be apparently prolate due to errors in axial ratio measurements resulting in highly erroneous V estimates.

If the errors of Es and V estimates are large, then true oblate or semi-plane strains may be incorrectly represented by the prolate Es/V plots. If this were the case, a plane strain may have been superimposed on an oblate strain with identical principal axes orientations. Therefore, with increasing magnitudes of plane strain, the finite strain's approach plane strain, but never attain prolate values. However the prolate strains measured in the field are most likely realistic as the error triangle of sample 2 (Figure 8A) suggests.

(b) Secondly, the division of the finite strains into two separate incremental strains which are related to two distinct deformations may not be valid. The low Ri values obtained by Rf/Ø diagram analysis suggest only one deformation has been imposed on initial sedimentary fabrics.

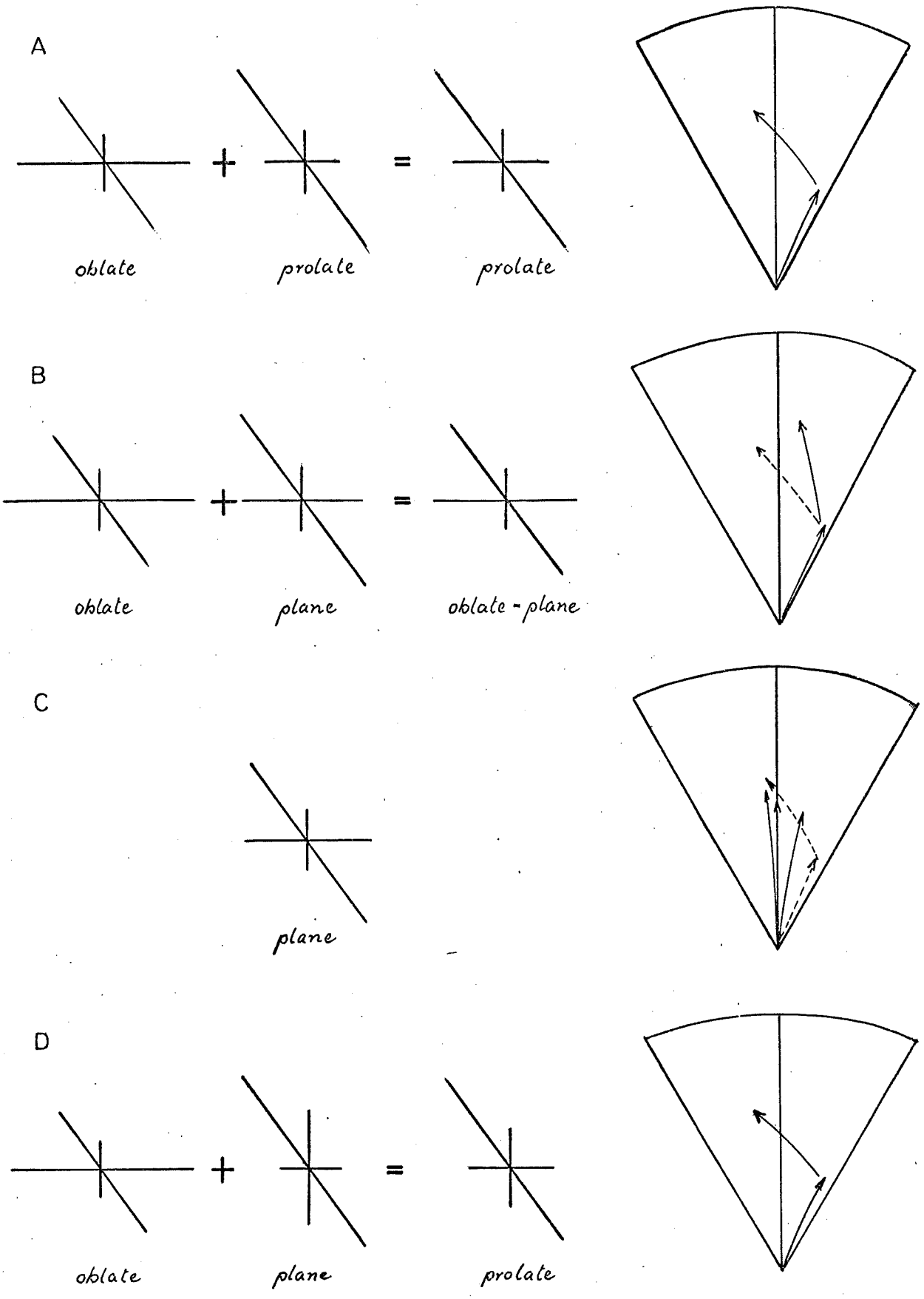

FIGURE 10. DEFORMATION PATHS: Alternative Interpretations

A. Finite strain variation represents true deformation paths. Prolate on oblate strains.

B. Prolate strain estimates erroneous. Plane on oblate strains.

C. Oblate strain estimates erroneous. Single plane strain deformation.

D. Finite strain variation represents true deformation paths. Plane strain on oblate strain with reversed Y and Z axes.

The trend of the variation of the finite strains may only be apparent due to errors in strain measurement producing anomalous oblate strains for low Es values. If this were the case, then a single plane strain deformation may have produced the observed variation of estimated finite strains (Figure 10).

The consistent linear trend of estimated finite strains, however, suggests it is representative of the true strain variation. The inferred oblate strain may not be real and therefore, the fold formation is genetically inseparable from the formation of the zones of intense shearing. In response to a single deformation, the spread of finite strain values may develop due to strain inhomogeneity throughout the conglomerate and not by a progressive deformation from oblate to prolate strains. Therefore, the Es/V plots represents the finite strains of a number of deformation paths, which probably radiate from approximately zero Es and V values which represent the strains of initial sedimentary fabrics (Figure 10).

In view of the consistent linear trend of the finite strain variation on the Es/V diagram and the real existence of prolate strains in the area, it is considered that a true plane strain due to simple shear did not produce the finite strains in the conglomerate. As the formation of the elongation lineation is considered contemporaneous with the LS fabric development, there are two possible relationships between the basement and cover deformations.

(a) The simple shear mechanism proposed for the zone along the basement-cover contact of the overturned limb may be invalid. Therefore the same deformation mechanism, which produced the prolate strain, may apply to both the cover and basement.

(b) Alternatively, the simple shear model may apply to the basement on the overturned limb, but a different response of the cover lithologies to the deformation may have caused the change in

strain symmetry across the basement-cover contact. This explains the greater phyllonitization and foliation development in the basement lithologies.

Alternative (a) is preferred, as the determination of prolate strains by axial ratio measurements is more quantitative than the inference of plane strain by the existence of zones of LS fabric development and by the macroscopic variation of fabric orientations. Also the change from one deformation mechanism to another between different lithologies requires a complex stress situation in the transition zone between the two mechanisms.

6. LATER DEFORMATIONS

Two minor deformations followed the development of the LS fabric. As the resulting structures are small-scale and not persistent throughout the area, the relative ages of the two deformations are not determinable.

6.1 Crenulation Cleavage and Lineation

Small scale mesoscopic crenulation of the foliation is related to a crenulation lineation which has a shallow pitch to the east within the foliation (Plate 2). By their nature and orientation, these structures are correlated with the F_2 structures described by Daily and Milnes (1973) on the eastern side of Fleurieu Peninsula.

The crenulation occurs predominantly in the highly deformed, thinly foliated basement lithologies. In the mylonitic chlorite schists, small planar zones of reoriented foliation strike approximately west to southwest and dip 15 degrees to the northwest. Due to the irregularity of the crenulations, the orientation of the superimposed cleavage is difficult to determine.

The associated crenulation lineation is best developed as a fine regular wrinkling on the planes of slaty cleavage within the cover units.

6.2 Conjugate Faulting and Associated Fold Development

Two sets of fault planes form a conjugate set with the acute angle between the two fault trends orientated to the southeast. The faults are generally steeply inclined, but the dips of the fault planes were not determined.

Normal movements along the faults has produced angular monoclinal and conjugate folds in the thinly foliated Tapley Hill Formation on the west limb (Plate 1). This style of folding is similar to the "joint drags" described by Flinn (1952). Displacements along the faults vary from very small movements to displacements of several

metres. The scale of the folding varies from conjugate folds less than .5 metres wide to cleavage and bedding warps over 100 metres in extent as seen in the cliffs immediately north of Second Valley harbour.

7. CONCLUSIONS

7.1 General

In the nose of the Myponga-little Gorge Inlier, the F_1 phase of the Delamerian Orogeny is characterized by three effects, viz. the formation of the regional overturned fold, the development of a prolate strain in the cover and phyllonitization of basement, and to a lesser degree, of cover lithologies adjacent to the basement-cover contact on the overturned limb.

The regional fold closes to the southwest around the nose of the basement inlier. Parasitic mesoscopic folds are reclined with fold axes plunging southeast down the dip of the axial plane foliation. The regional fold is therefore reclined.

7.2 Nature of Deformation

An elongation lineation is developed sub-parallel to the mesoscopic fold axes. Strain analysis of the basal conglomeratic unit indicate a linear trend of finite strain variation from oblateness to prolateness with increasing magnitude of strain. If the trend is considered to be representative of a deformation path during progressive deformation, then two phases of deformation may be proposed, whereby a prolate strain is superimposed on an oblate strain which developed during the regional folding. However Rf/Ø diagram analysis suggests the quartz grain and pebble fabrics were sedimentary prior to the deformation which produced the prolate finite strains. Therefore the development of the elongation lineation may be contemporaneous with, or post-date the formation of the regional fold.

An LS fabric is developed in planar zones of intense deformation, which parallel the basement-cover contact of the west limb. A model of simple shear is proposed to explain the observed variation in fabric orientation within these zones. The shear directions of the model indicate thrusting of the basement along the basement-cover contact.

The development of the elongation lineation is contemporaneous with the formation of the foliation in the shear zones. Therefore the estimates of prolate strain in the conglomerate conflict with the plane strain suggested by the simple shear model. As the determination of the finite strains in the conglomerate is quantitative and the trend of the finite strain variations is well defined, a prolate strain is considered to have developed during the deformation which caused the phyllonitization of the basement and cover lithologies. Therefore, the simple shear model of the planar zones of deformation may not be valid.

7.3 Relationship of Fold Formation to Elongation Lineation Development

If the formation of the elongation lineation is assumed to post-date the regional fold formation, then the sub-parallelism of the mesoscopic fold axes with the lineation needs to be explained. Elsewhere in the Mount Lofty Fold Belt, the regional fold axes commonly have shallow plunges to the north and south within the axial plane and are not reclined. Therefore the X axis of the strain ellipsoid associated with the fold formation is generally steeply plunging within the axial plane and it approximately parallels the elongation lineation in the Second Valley area.

Consequently, it is possible that the mesoscopic and macroscopic fold axes, after initial formation, are rotated within the axial plane into parallelism with the X direction of the prolate strain. Rotation of linear elements to a preferred orientation about the X elongation direction is theoretically possible by both pure shear (Sanderson, 1972) and simple shear (Escher and Watterson, 1974). As the strains are considered to be prolate, the fold reorientation is considered to occur by irrotational pure shear.

The low scatter and close parallelism of the fold axes to the X direction of the elongation lineations suggest either high

strains or a low initial angle (θ) between the fold axes and X direction within the XY axial plane. Sanderson derives the theoretical variation of θ with increasing strain ($^{X}/_{Y}$) (Sanderson, (op.cit.), figure 1). The highest $^{X}/_{Y}$ ratios obtained in the conglomerate are approximately 5:1. Therefore, for an $^{X}/_{Y}$ strain of 5, an initial θ less than 25 degrees is required to obtain final θ values less than 5 degrees. This suggests either (a) a steep initial fold axis plunge within the axial plane existed at the time of fold formation; (b) the magnitude of the deformation which produced the elongation lineation is not sufficient to rotate the macroscopic fold axis into parallelism with the X principal direction; or (c) the development of the elongation lineation is genetically related to the fold formation, during which the fold axis is orientated parallel to the X principal direction of the strain ellipsoid.

7.4 Recommendations

Further quantitative data is required to determine the relationship of the cover and basement deformations. If suitable strain markers can be used, then strain analysis of basement lithologies may reveal the strain variation across the basement-cover contact. Additional strain measurements of the conglomerate and also of the Sturt Tillite, are needed to develop a better understanding of the nature of the finite strains in the cover lithologies.

Evidence of the relationship between the regional fold formation and the development of the elongation lineation is inconclusive. In addition to strain analysis, this problem may be further investigated by morphological studies of the numerous mesoscopic folds in the area. Determination of the extent of shortening across the XY planes of the folds will add to the quantitative data available.

Plate 3

(1) View southwest along the coastal cliffs. Second Valley jetty and Rapid Bay quarry are in the distant background. The Congeratinga River outlet is centre left.

(2) Pebble of banded gneiss in the Sturt Tillite, northeast of Second Valley jetty.

(3) Basal conglomerate unconformably overlying basement schists on the overturned west limb. Pebbles are flattened in the foliation. Location 5, YZ plane, Little Gorge Beach.

(4) High angle between the fold envelope and the foliation (parallel to hammer) in the Burra Group, east limb. Congeratinga River outlet.

1

2

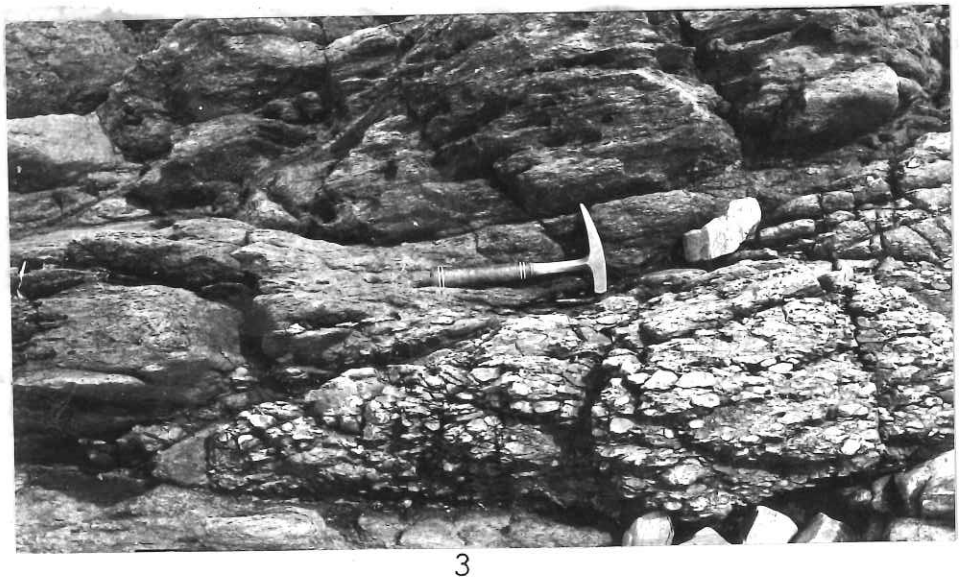

3

4

Plate 4

(1) Quartz filled microfault which parallels the regional thrusts. Burra Group, Congeratinga River outlet.

(2) Monoclinal folding of bedding and foliation associated with a minor fault. Tapley Hill Formation, Second Valley jetty area.

(3) Intense foliation in basement chloritic schists. F_2 crenulation of the foliation occurs in distinct zones. Congeratinga River outlet.

1 Photo messie

2

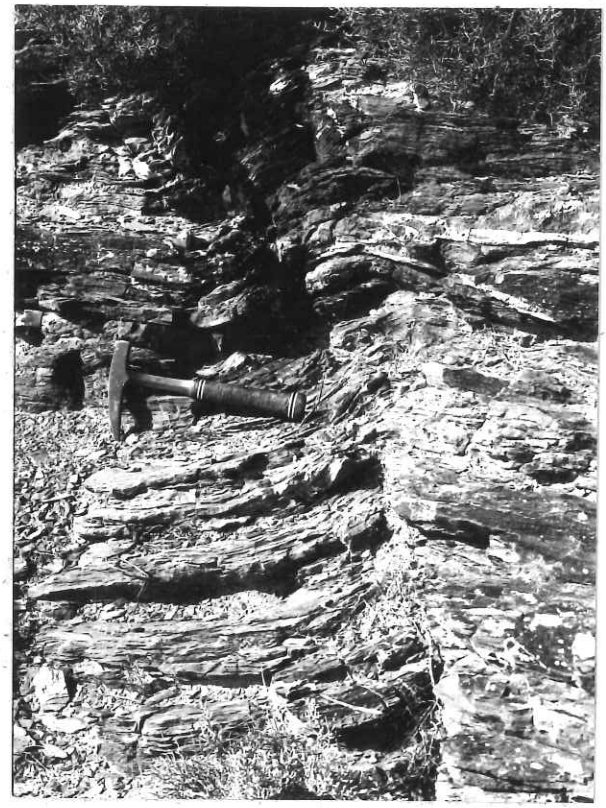

3

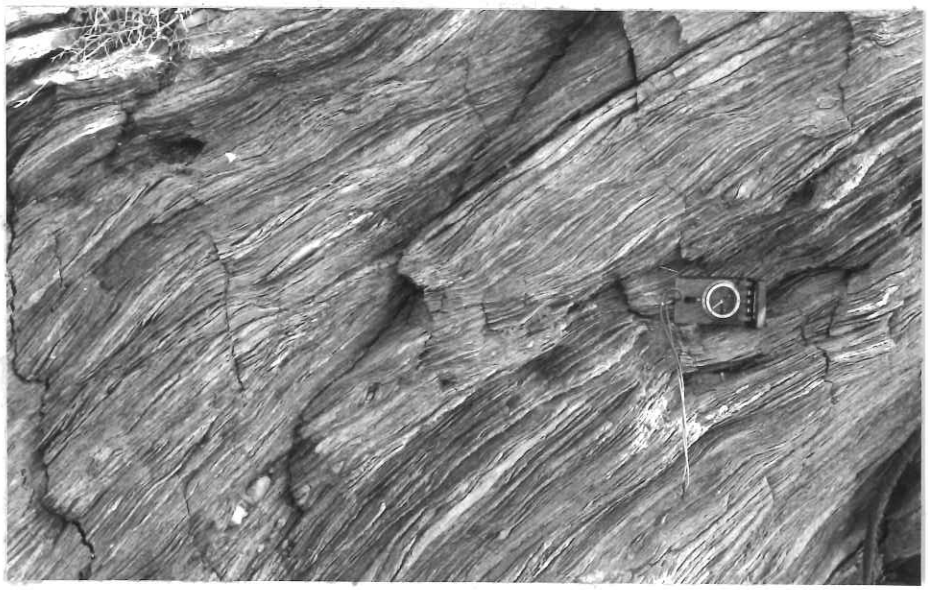

Plate 5

(1) XZ principal plane of the deformed conglomerate. The pebbles are rotated and flattened into the cleavage trace (parallel to hammer handle). Location 3, Little Gorge Beach.

(2) XY principal plane Location 5, Little Gorge Beach.

(3) XZ principal plane Location 3, Little Gorge Beach.

Photo missing

1

2

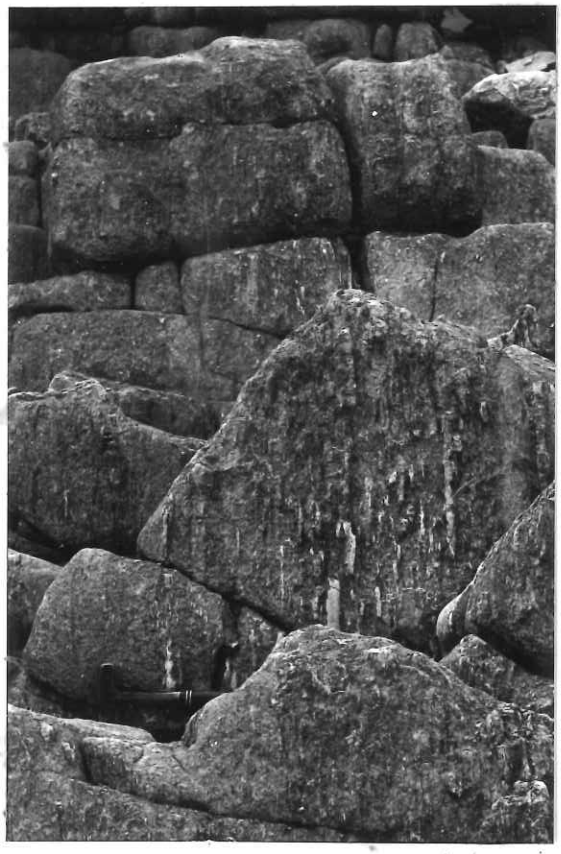

3

Plate 6

(1) Ribbons of recrystallized quartz and elongate relict quartz grains paralleling the foliation in the sericite matrix. Basement sericite schists, Anacotilla River. Crossed polars, 30X.

(2) Strings of recrystallized subpolygonal quartz in a sericite and chlorite matrix. Scattered idioblastic opaque grains also occur in the matrix. Basement chloritic schists, Congeratinga River outlet. Crossed polars, 30X.

(3) Fractures approximately 45^{o} to the elongation direction in a feldspar grain. Basement sericite schists, Little Gorge Beach. Crossed polars, 30X.

(4) Deformed basal arkosic sandstone. The quartz is undulose, elongate and recrystallizing, whereas the smaller feldspar grains are more equant. Crossed polars, 30X.

(5) Deformed basal arkosic sandstone. Plane polars, 30X. Deformed detrital shapes surrounded by growing sericite.

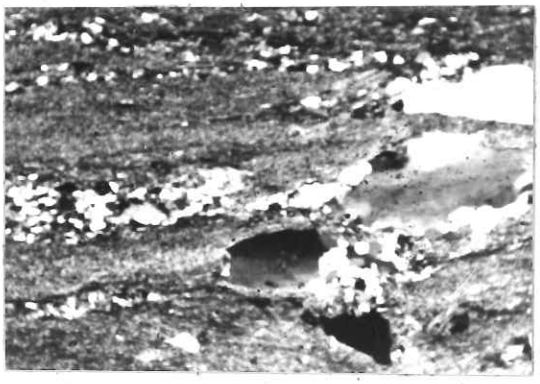

1

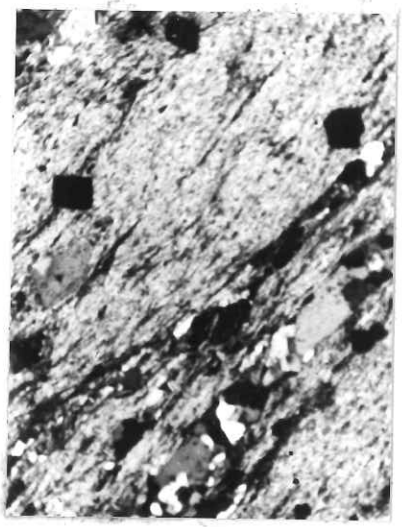

2

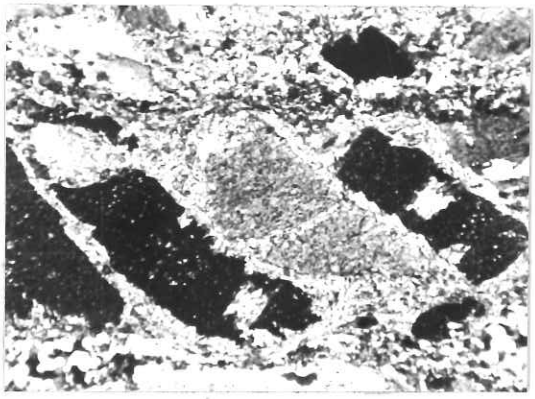

3

4

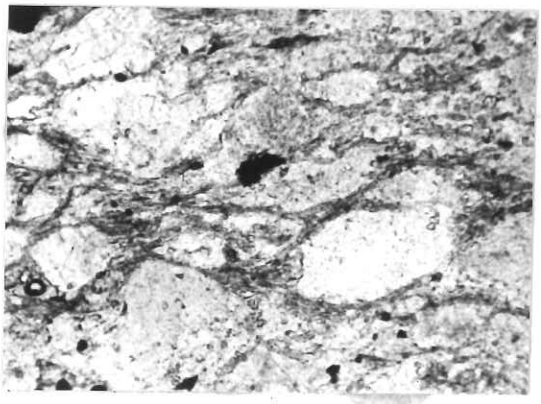

5

ACKNOWLEDGEMENTS

I gratefully acknowledge the supervision of Professor R.W.R. Rutland and Dr. P.R. James during the year. Assistance was also received from other members of the department's academic and technical staff, including Dr. R.L. Oliver and Dr. B. Daily. In particular, I wish to thank N. Manchtelow, a research student of the department, for invaluable comments and criticism.

BIBLIOGRAPHY

Abele, C., and McGowran, B., 1959. The geology of the Cambrian south of Adelaide (Sellick Hill to Yankalilla). *Trans. R. Soc. S. Aust., 82*: 301-320.

Barber, A.J., and Soper, N.J., 1973. Summer Field Meeting in the North-West of Scotland. *Proc. Geol. Ass. Lond., 84*: 207-235.

Bell, T.H., and Etheridge, M.A., 1973. Microstructure of Mylonites and their descriptive terminology. *Lithos, 6*: 337-348.

Campana, B., Wilson, R.B., and Whittle, A.W.G., 1953. The geology of the Jervis and Yankalilla military sheets. Geological Survey of South Aust; *Rpt. Invest. No. 3.*

Carter, N.L., Christie, J.M., and Griggs, D.T., 1964. Experimental deformation and recrystallization of quartz. *Jour. Geology, 72*: 687-733.

Christie, J.M., 1960. Mylonitic Rocks of the Moine Thrust-Zone in the Assynt Region, North-West Scotland. *Edinb. Geol. Soc. Trans., 18*: 79-93.

Cloos, E., 1947. Oolite deformation in the South Mountain Fold, Maryland. *Bull. geol. Soc. Am., 58*: 843-918.

Compston, W., Crawford, A.R., and Bofinger, F.M., 1966. A radiometric estimate of the duration of sedimentation in the Adelaide Geosyncline, South Australia. *J. geol. Soc. Aust., 13 (1)*: 229-276.

Daily, B., 1963. The fossiliferous Cambrian succession on Fleurieu Peninsula, South Australia. *Rec. S. Aust. Mus., 14 (3)*: 579-601.

Daily, B., and Milnes, A.R., 1971a. Stratigraphic notes on Lower Cambrian fossiliferous metasediments between Campbell Creek and Tunkalilla Beach in the type section of the Kanmantoo Group, Fleurieu Peninsula, South Australia. *Trans. R. Soc. S. Aust., 95 (4)*: 199-214.

Daily, B., and Milnes, A.R., 1971b. Discovery of Late Precambrian Tillites (Sturt Group) and Younger Metasediments (Marino Group) on Dudley Peninsula, Kangaroo Island, South Australia. *Search, 2 (11-12)*: 431-433.

Daily, B., and Milnes, A.R., 1972a. Significance of basal Cambrian Metasediments of andalusite grade, Dudley Peninsula, Kangaroo Island, South Australia. *Search, 3 (3)*: 89-90.

Daily, B., and Milnes, A.R., 1973. Stratigraphy, structure and metamorphism of the Kanmantoo Group (Cambrian) in its type section east of Tunkalilla Beach, South Australia. *Trans. R. Soc. S. Aust., 97 (3)*: 213-242.

Davies, M.B., 1972. A. The geology and petrology of an Archaean Inlier South of Normanville. B. The geochemistry of the "Houghton" granulite. Unpublished thesis, University of Adelaide.

Drayton, R.D., 1962. The structural geology of the Rapid Bay Area. Unpublished thesis, University of Adelaide.

Dunnet, D., 1969. A technique of finite strain analysis using elliptical particles. *Tectonophysics, 7 (2)*: 117-136.

Dunnet, D., and Siddans, A.W.B., 1971. Non-random sedimentary fabrics and their modification by strain. *Tectonophysics, 12*: 307-325.

Escher, A., and Watterson, J., 1974. Stretching fabrics, folds and crustal shortening. *Tectonophysics, 22*: 223-231.

Flinn, D., 1952. A tectonic analysis of the Muness Phyllite Block of Unst and Uyea, Shetland. *Geol. Mag., 89*: 263-272.

Flinn, D., 1965. On the symmetry principle in the deformation ellipsoid. *Geol. Mag., 102*: 36-45.

Forbes, B.G., 1966. Features of Palaeozoic tectonism in South Australia. *Trans. Roy. Soc. S. Aust., 90*: 45-56.

Gay, N.C., 1968a. Pure shear and simple shear deformation of inhomogeneous viscous fluids. 1. Theory. *Tectonophysics, 5(3):* 211-234.

Gay, N.C., 1968b. Pure shear and simple shear deformation of inhomogeneous viscous fluids. 2. The determination of the total finite strain in a rock from objects such as deformed pebbles. *Tectonophysics, 5 (4)*: 295-302.

Hossack, J.R., 1968. Pebble deformation and thrusting in the Bygdin area (Southern Norway). *Tectonophysics, 5 (4)*: 315-339.

Kleeman, A.W., and White, A.J.R., 1956. The structural petrology of portion of the eastern Mt. Lofty Ranges. *J. geol. Soc. Aust., 3*: 17-31.

Knill, J.L., 1960. Joint Drags in Mid-Argyllshire. *Proc. Geol. Ass. Lond., 72*: 13-19.

McEwin, A.J., 1972. Geology and petrology of part of the Archaean inlier north-east of Yankalilla, Fleurieu Peninsula. Unpublished thesis, University of Adelaide.

Milnes, A.R., 1973. The Encounter Bay Granites, South Australia, and their environment. Unpublished thesis, University of Adelaide.

Offler, R., and Fleming, P.D., 1968. A synthesis of folding and metamorphism in the Mt. Lofty Ranges, South Australia. *J. geol. Soc. Aust., 15 (2)*: 245-266.

Parkin, L.W., 1969. Handbook of South Australian geology. Geological Survey of South Australia.

Phemister, J., 1960. Scotland: The Northern Highlands (3rd. edition). Natural Environment Research Council Institute of Geological Studies.

Ramsay, J.G., 1967. Folding and fracturing of rocks. McGraw-Hill Book Company.

Ramsay, J.G., and Graham, R.H., 1970. Strain variation in shear belts. *Canadian Journal of Earth Sciences, 7*: 786-813.

Robinson, W.B., 1962. The geology of the Normanville-Second Valley area. Unpublished thesis, University of Adelaide.

Sanderson, D.J., 1973. The development of fold axes oblique to the regional trend. *Tectonophysics, 16*: 55-70.

Sprigg, R.C., and Campana, B., 1953. The age and facies of the Kanmantoo Group. *Aust. J. Sci., 16 (1)*: 12-14.

Stuart, W.J., and von Sanden, A.T., 1972. Palaeozoic history of the St. Vincent Gulf region, South Australia. *A.P.E.A. Jour.* 9-16.

Talbot, J.L., 1964. The structural geometry of rocks of the Torrens Group near Adelaide, South Australia. *J. geol. Soc. Aust., 11*: 33-48.

Thomson, B.P., 1966. The lower boundary of the Adelaide System and older basement relationships in South Australia. *J. geol. Soc. Aust., 13 (1)*: 203-228.

Williams, K., 1975. Deformation, recovery, polygonlization, recrystallization and grain growth. Printed notes presented at University of Adelaide, Oct. 1-3, 1975.

APPENDIX 1. THIN SECTION DESCRIPTIONS

COVER LITHOLOGIES

Description No. 1 - 455/NC3 (XZ section)

Field name: Basal arkosic sandstone (Aldgate Sandstone)

Macroscopic: Coarse grained, micaceous, feldspathic sandstone. Thin sedimentary bands of heavy mineral grains separate thicker bands of coarse pink feldspar and quartz. A good lineation and foliation development.

Microscopic: Lenticular zones of strained relict quartz and fine recrystallized quartz separated by bands of very fine lepidioblastic sericite. High degree of recrystallization to fine polygonal quartz. Relict quartz strongly undulose and xenoblastic. Detrital feldspar grains are fractured and kinked.

Relict quartz	- 10%; 1-5 mm
Recrystallized quartz	- 40%; .075 mm
Feldspar	- 25%; 1-6 mm; Ab and Ab/pericline twinning.
Sericite	- 25%; very fine
Opaque detrital grains	- 2%; fine.

Description No. 2 - 455/G2 (YZ section)

Field name: Basal arkosic sandstone (Aldgate Sandstone)

Macroscopic: Very micaceous, light coloured, feldspathic sandstone. Faint heavy mineral layering. Well foliated.

Mesoscopic: Initial sedimentary quartz completely recrystallized. Original sedimentary grainsize is 1-2 mm. Coarse feldspars fractured approx. 45 degrees to foliation. Original sedimentary grain concentration is 75%.

Recrystallized quartz	- 60%; .1-.3 mm
Feldspar	- 5%; .7-4 mm; Ab/pericline twinning
Sericite	- 30%
Ilmenite	- 2%; .25 mm

Description No. 3 - 455/M30

Field name: Interbanded indurated siltstone (Burra Group)

Microscopic: Original sedimentary banding defined by regular bands of coarse quartz, carbonate and biotite alternating with bands of finer quartz and higher biotite concentration. Quartz and carbonate is recrystallized. Lepidioblastic biotite defines foliation. Chlorite growing sub-parallel to the foliation in the zones of coarse quartz.

Recrystallized quartz	- 40%; bimodal .05-.15 mm and .25 mm.
Biotite	- 25%; .05 mm; brown to green.
Chlorite	- 20%; .2 mm
Muscovite	- 2%; .1 mm
Carbonate	- 10%
Opaques	- 3%

Very fine, calcareous, biotite, chlorite metaquartzite interbanded with a coarse, calcareous, biotite metasiltstone.

Description No. 4 - 455/31C10

Field name: Crenulated chlorite, sericite schist (Tapley Hill Formation)

Microscopic: Alternating bands (approximately .5-4 mm wide) of sericite with coarser quartz and chlorite. Foliation developed by lepidioblastic sericite. Quartz varies in nature from interlocking to isolated grains in micaceous host and is sub-parallel to the foliation. Foliation is microcrenulated.

Quartz	- 50%; .07 mm or .1-.2 mm
Chlorite	- 15%; .05-.07 mm
Sericite	- 25%; v. fine
Opaques	- 5%; .07 mm

Description No. 5 - 455/17C20

Field name: Feldspathic quartzite pebble from basal conglomeratic sandstone (Aldgate Sandstone).

Macroscopic: Elongated and flattened quartzite pebble. Medium-fine quartz and pink feldspar. Fine scattered opaque grains. Homogeneous. Slightly micaceous.

Microscopic: Ragged undulose quartz and equant feldspar grains. Quartz slightly flattened in XY plane of pebble and is extensively recrystallized to polygonal, finer quartz. Slight foliation development due to sericitization of feldspar.

Relict quartz	- 25%; 1-2 mm
Recrystallized quartz	- 50%; .1-.3 mm
Feldspar	- 15%; .3-.5 mm
Sericite	- 4%;
Opaques	- 2%; v.fine- .4 mm
Sphene	- common accessory; .05 mm

BASEMENT LITHOLOGIES

Description No. 6 - 455/J11

Field name: Quartz feldspar Biotite gneissic schist.

Macroscopic: Granitoid zones of coarse, pink feldspar, quartz and biotite are separated by more schistose biotite rich layers.

Microscopic: Relict granoblastic texture of coarse quartz, feldspar and biotite is disrupted by sericitization and quartz recrystallization. Quartz moderately undulose but quartz and feldspar grains are not highly fractured. Brown biotite is altering to green biotite and possibly to minor chlorite. Recrystallization of quartz is not extensive.

Relict quartz	- 20%; 2-12 mm
Recrystallized quartz	- 5%
Feldspar	- 45%; 1.5-8 mm
Biotite	- 5%; 1-2 mm
Chlorite	- 1%; .15 mm
Epidote	- 5%; .25 mm
Sericite	- 20%
Opaques - accessory	

Description No. 7 - 455/21B1

Field name: Medium grained quartz, feldspar, biotite schist.

Macroscopic: bands of quartz and feldspar alternating with more biotite rich layers approx. .5 cm wide.

Mesoscopic: Alternating quartz/biotite and quartz/feldspar layers are approx. .5-1.0 cm. wide. Biotite is sublepidioblastic resulting in a weak foliation at an angle to the layering. Quartz is slightly flattened parallel to the foliation and is strongly undulose.

Feldspar	- 35%; .15-2 mm
Relict quartz	- 15%; .2-.5 mm
Recrystallized quartz	- 5%; .05-.2 mm
Biotite	- 35%; .05- 1 mm
Epidote	- 1%; .2- 1 mm
Sericite	- 10%; fine
Opaques	- 3%; .05-.5 mm

Description No. 8 - 455/I4

Field name: Quartz, feldspar, sericite schist.

Macroscopic: Light coloured schistose rock with brown and green tinge. Pink feldspar and coarse grey quartz are slightly flattened in the foliation. Well developed lineation by mineral streaking.

Microscopic: Lenticles of recrystallized quartz and xenoblastic feldspars are elongate parallel to the lepidioblastic sericite and biotite matrix. Biotite is altering to iron oxides. Chlorite is crystallizing with the polygonal quartz growth. Feldspars are fractured at high angle to the foliation.

Recrystallized quartz	- 20%; .075 mm
Feldspars	- 20%; .5-5 mm
Sericite	- 45%, v. fine
Biotite	- 3%; .2 mm
Opaques	- 5%; .5 mm
Tourmaline	- accessory
Zircon	- accessory

Description No. 9 - 455/20B1

Field name: Biotite, sericite quartz schist.

Macroscopic: Fractured and embayed quartz and feldspar with recrystallized, fine unstrained polygonal quartz as stringers and bands separated by fine sericite and coarser green biotite bands. Sericite infills high angle fractures in feldspars. Micas are lepidioblastic, sericite more so than biotite. Opaques are uniformly scattered throughout.

Relict quartz	- 15%; .5-1.5 mm
Recrystallized quartz	- 15%; .075-.2 mm
Feldspar	- 20%; .3-2 mm; no twin lamellae
Sericite	- 45%
Biotite	- 7%; .4 mm
Opaques	- 3%; .4 mm
Zircon	- accessory
Tourmaline	- accessory

Description No. 10 - 455/3B10

Field name: Chlorite, sericite, quartz schist. ("Oystershell Rock")

Macroscopic: Schistose green rock with irregular foliation surfaces. Stringers and lenticles of grey quartz are flattened in foliation.

Microscopic: Lenticular augen of relict medium grained quartz in fine, even-grained, lepidioblastic sericite matrix. Considerable re-

crystallization to fine polygonal quartz. Fractures in quartz at approx. 45 degrees to the foliation are infilled by fine quartz and sericite.

Relict quartz	- 15%; 2.0 mm
Recrystallized quartz	- 20%; .05 mm
Feldspar	- 2%; 1.0 mm; no twin lamellae
Sericite	- 55%
Chlorite	- 7%; .07 - .2 mm
Tourmaline	- 5%; .07 - .3 mm
Muscovite	- 3%; .15 mm
Opaques	- 3%; .05 mm
Zircon	- accessory

Description No. 11 - 455/021

Field name: Augen schist. ("Flaser Gneiss")

Macroscopic: Lenticular bands of medium grained pink feldspar and quartz in a fine foliated groundmass of feldspar, quartz and sericite. Microscopic - lenticular bands of relict and sub-polygonal recrystallized quartz and feldspars, .1 - 1.0 cm wide. Interfoliated by lepidioblastic sericite bands approx. .3-1 mm wide. Feldspar is kinked, fractured and sericitized. Quartz is flattened, undulose and largely recrystallized.

Relict quartz	- 5%; .5-1.0 mm
Recrystallized quartz	- 40%; .05-.5 mm
Microcline	- 10%; .15-5.0 mm
Sericite	- 40%
Opaques	- 5%; .08 mm
Zircon	- accessory
Tourmaline	- accessory.

APPENDIX 2. TABULATED DESCRIPTION OF SAMPLES USED FOR QUARTZ GRAIN STRAIN ANALYSIS

Location numbers refer to Plate 1.

Constituent concentrations in percent of total rock.

Dash - no data available.

Field No.	Location No.	Relict Qtz.	Recrystallized Qtz.	Feldspar	Sericite	Grain size Ave. detrital
455/2C6	1	25	30	25	20	1.75
" 3C11	3	-	-	-	-	-
" 7C1	6	40	20	10	30	2.0
" 8C2	7	25	20	20	30	1.5
" NC2	9	25	25	10	40	3.0
" NC3	10	10	45	20	25	3.0
" M3	11	-	-	-	-	-
" M6	12	30	-	20	-	1.75
" I1	13	-	-	-	-	1.5
" G4	14	25	35	20	10	1.75
" G1	15	10	40	25	20	1.5
" G2	16	0	65	5	25	1.5
" E1	17	50	10	10	25	2.0
" A1	19	35	40	10	5	2.0
" 16C17	21	15	30	20	30	2.5
" 17C7	23	15	25	20	40	1.0
" 17C8	24	-	-	-	-	-
" 17C10	25	25	20	15	30	2.0
" 20C1	26	25	45	20	5	1.5

GEOLOGICAL MAP OF THE SECOND VALLEY - LITTLE GORGE AREA

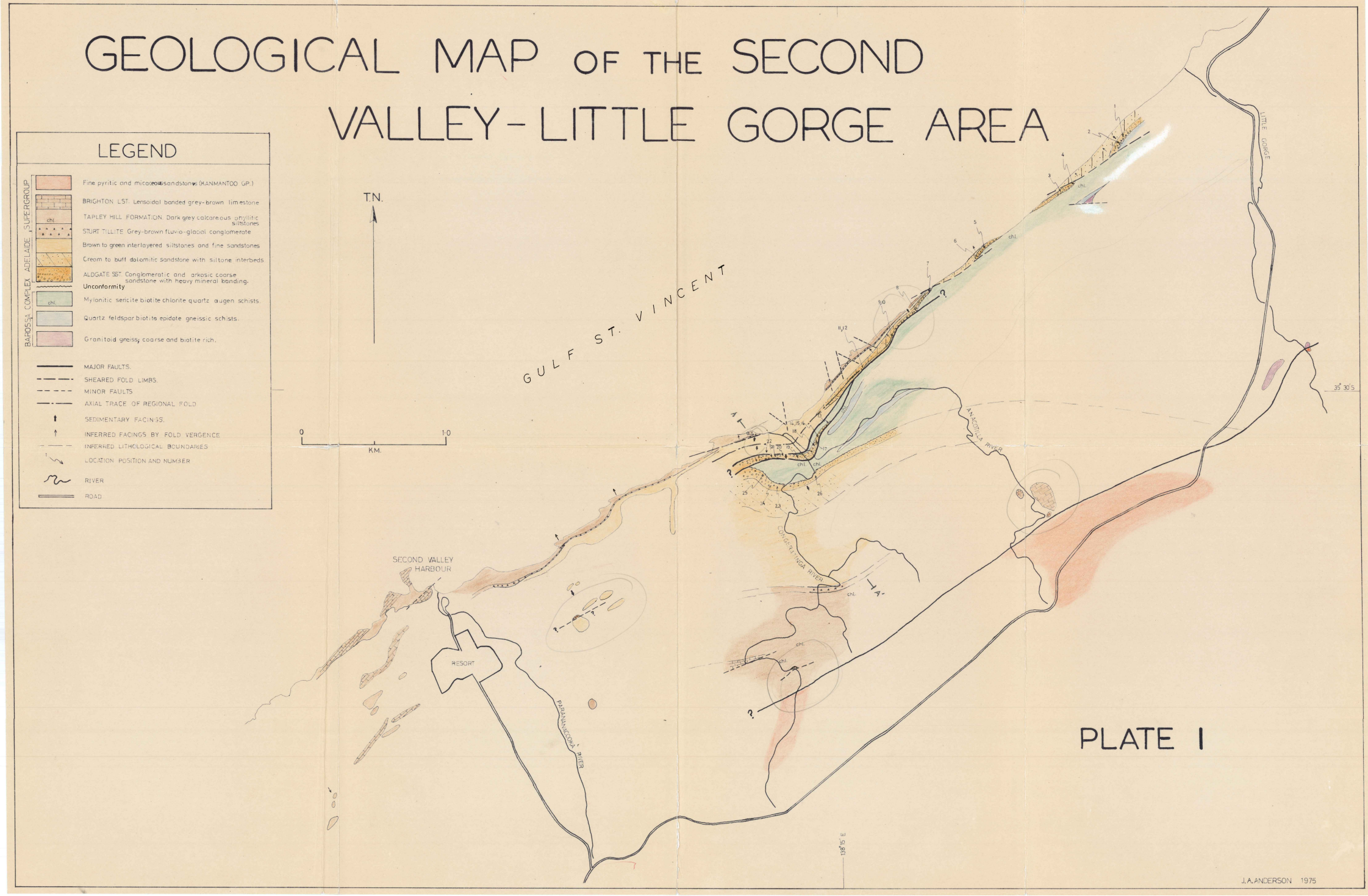

PLATE 2. EQUAL AREA STEREONET PROJECTIONS

(COUNTING CELL AREA = 2%)

POLES TO BEDDING

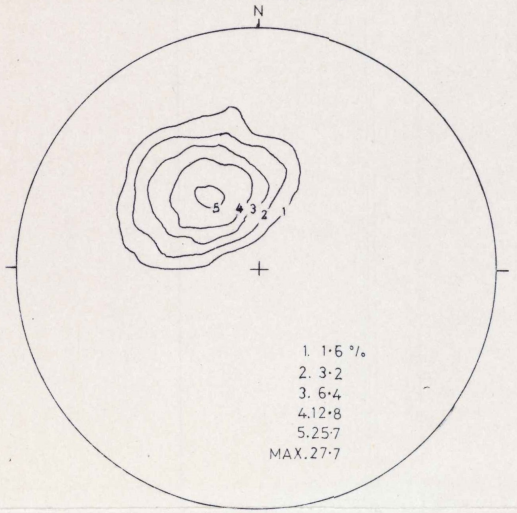

(Nº OF ORIENTATIONS = 146)

POLES TO COVER FOLIATION

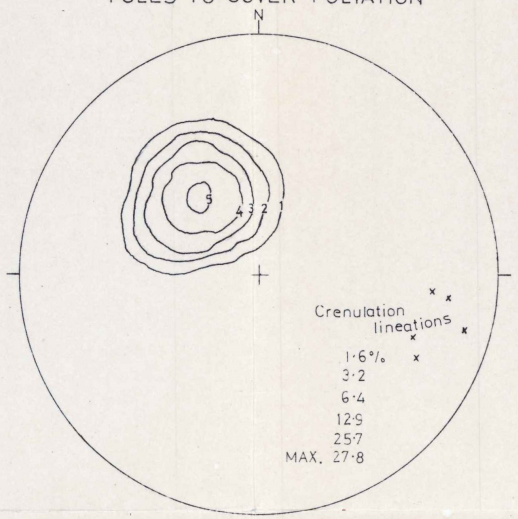

(268)

POLES TO BASEMENT FOLIATION

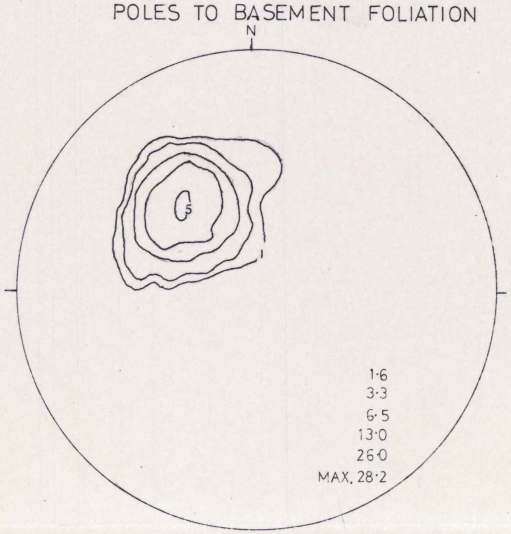

(151)

POLES TO SMALL SCALE FAULTING

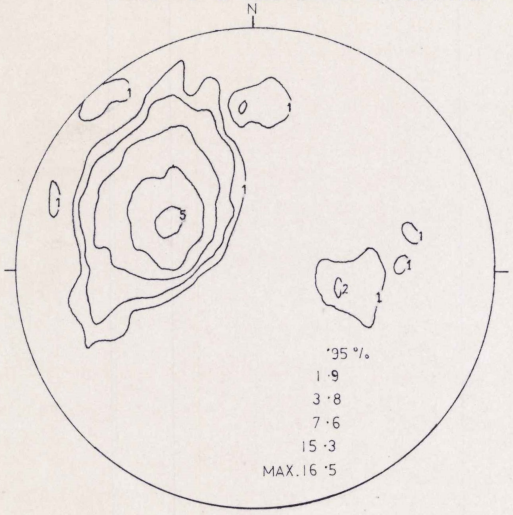

(103)

COVER LINEATIONS

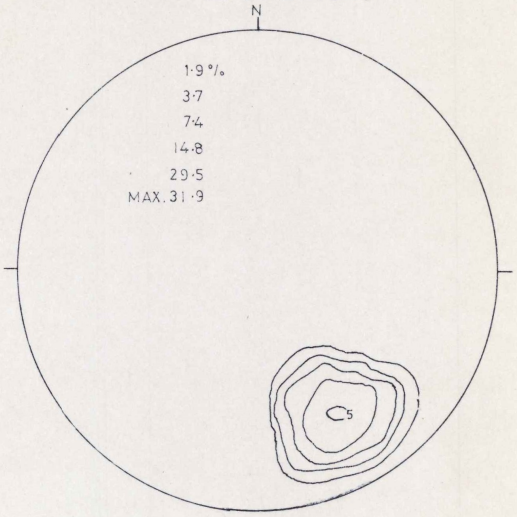

(202)

BASEMENT LINEATIONS

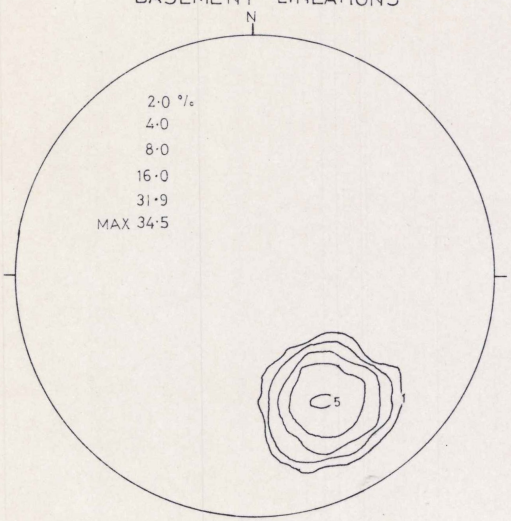

(113)

FOLD AXES

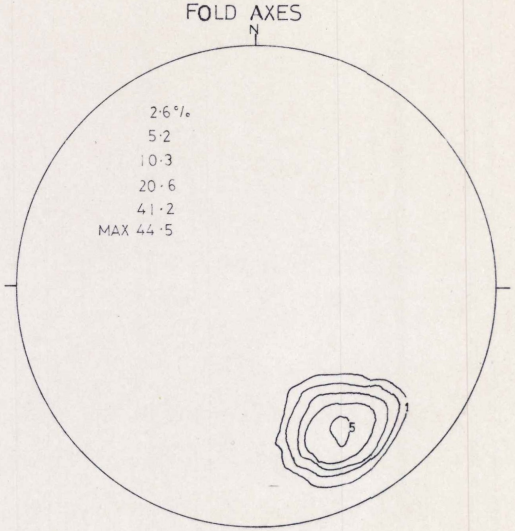

(46)

J.A.A. 1975